



**US Army Corps
of Engineers®**
Engineer Research and
Development Center

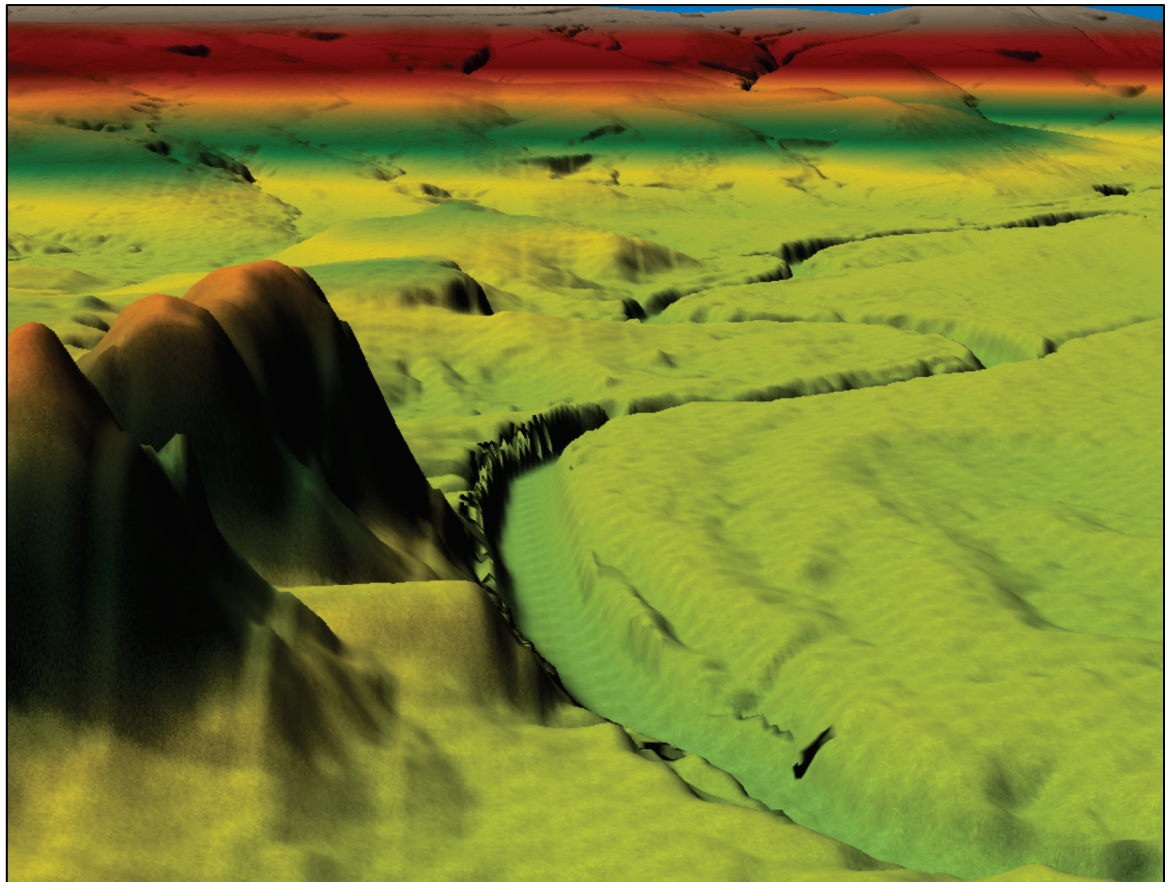


Wetlands Regulatory Assistance Program (WRAP)

Hydrologic Analysis of Field Delineated Ordinary High Water Marks for Rivers and Streams

Daniel Hamill and Gabrielle C. L. David

August 2021



The US Army Engineer Research and Development Center (ERDC) solves the nation's toughest engineering and environmental challenges. ERDC develops innovative solutions in civil and military engineering, geospatial sciences, water resources, and environmental sciences for the Army, the Department of Defense, civilian agencies, and our nation's public good. Find out more at www.erdclibrary.on.worldcat.org/discovery.

To search for other technical reports published by ERDC, visit the ERDC online library at www.erdclibrary.on.worldcat.org/discovery.

Hydrologic Analysis of Field Delineated Ordinary High Water Marks for Rivers and Streams

Daniel Hamill and Gabrielle C. L. David

*Cold Regions Research and Engineering Laboratory
US Army Engineer Research and Development Center
72 Lyme Road
Hanover, NH 03755-1290*

Final report

Approved for public release; distribution is unlimited.

Prepared for Wetland Regulatory Assistance Program
US Army Corps of Engineers
Vicksburg, MS 39180-6933

Under Funding Account Code U4375873; AMSCO Code 088893

Abstract

Streamflow influences the distribution and organization of high water marks along rivers and streams in a landscape. The federal definition of ordinary high water mark (OHWM) is defined by physical and vegetative field indicators that are used to identify inundation extents of *ordinary* high water levels without any reference to the relationship between streamflow and regulatory definition. Streamflow is the amount, or volume, of water that moves through a stream per unit time. This study explores regional characteristics and relationships between field-delineated OHWMs and frequency-magnitude streamflow metrics derived from a flood frequency analysis. The elevation of OHWM is related to representative constant-level discharge return periods with national average return periods of 6.9 years using partial duration series and 2.8 years using annual maximum flood frequency approaches. The range in OHWM return periods is 0.5 to 9.08, and 1.05 to 11.01 years for peaks-over-threshold and annual maximum flood frequency methods, respectively. The range of OHWM return periods is consistent with the range found in national studies of return periods related to bankfull streamflow. Hydraulic models produced a statistically significant relationship between OHWM and bank-full, which reinforces the close relationship between the scientific concept and OHWM in most stream systems.

DISCLAIMER: The contents of this report are not to be used for advertising, publication, or promotional purposes. Citation of trade names does not constitute an official endorsement or approval of the use of such commercial products. All product names and trademarks cited are the property of their respective owners. The findings of this report are not to be construed as an official Department of the Army position unless so designated by other authorized documents.

DESTROY THIS REPORT WHEN NO LONGER NEEDED. DO NOT RETURN IT TO THE ORIGINATOR.

Contents

Abstract.....	ii
Figures and Tables.....	iv
Preface	vi
1 Introduction	1
1.1 Background	1
1.2 Objectives.....	9
1.3 Approach	9
2 Flood Frequency.....	12
2.1 Annual maximum (AM)	14
2.2 Peaks-over threshold (POT).....	15
2.2.1 Goodness-of-fit (GOF).....	17
2.2.2 POT threshold selection.....	18
2.3 Parameter estimation.....	20
3 Hydraulic Modeling Approach	22
3.1 Flow model formulation.....	22
3.2 Georeferencing	25
3.3 Calibration.....	26
4 Data Sources	27
4.1 Field surveys	27
4.2 Streamflow data	28
5 Hydrological Analysis of Ordinary High Water Mark (OHWM)	30
5.1 Case study northeast	30
5.1.1 Model description	33
5.1.2 OHWM delineation	34
5.1.3 Results.....	36
5.1.4 Implications of AM and POT flood frequency return periods.....	38
5.2 Flood frequency of OHWM	39
5.3 Relationships between bankfull discharge and OHWM	42
6 Summary.....	45
References.....	47
Acronyms and Abbreviations.....	52
Unit Conversion Factors.....	53
Report Documentation Page	

Figures and Tables

Figures

Figure 1. Conceptual diagram of flow classifications based on divisions that are of geomorphic and ecologic importance for a hypothetical cross section. The exact elevations bounding each flow category will vary based on channel type and various physical and vegetative indicators.	2
Figure 2. Bar graph of daily average streamflow record. The vertical red line shows the central tendency of the daily average streamflow record.	3
Figure 3. Labeled hydrograph identifying examples of flow events fitting within magnitude and frequency categories. Amounts of streamflow are described by the first term and the relative frequency.	4
Figure 4. Annual maximum return periods calculated for individual seasons and WYs. The return periods were calculated using the Weibull plotting position formula (return interval = $[N+1]/m$, where N is the number of years in streamflow record and m is the rank of each discharge value from largest to smallest. The color dots on the WY curve indicate which season the flooding event occurred.	9
Figure 5. National map showing the country divided into 8 geographic regions and 15 study sites (yellow stars with eight-letter site code) distributed across six of those regions.	10
Figure 6. Example showing differences between GP and LP3 statistical distributions for flood frequency analysis. The approximate thresholds for small-frequent, medium-intermediate, and large-infrequent flooding events are shown using rectangles with black outlines. The uncertainty bounds for each distribution are shown by the shaded regions.	14
Figure 7. Example of the FPOT filtering. Top panes show the daily discharge record with peaks and preceding flood minima. The lower panel shows a comparison of the FPOT and actual magnitude of the overall flooding event.	19
Figure 8. Example showing how GOF tests were used to identify a set of thresholds that are well described by the GP distribution. A suitable threshold for this example would exist between 600 and 800 cms because the τ and W2 are both less than the p-value.	20
Figure 9. Example cross section showing the horizontal variation of Manning's roughness.	24
Figure 10. Example cross section showing the vertical variation of Manning roughness values.	24
Figure 11. Example showing the merging process of survey points and collocated DEM derived cross section (XS).	26
Figure 12. Daily and peak streamflow period of record for OHWM survey sites. Gaps in the data, or particularly short records, meant that some of these sites were not suitable for the study (NEMJRPD, PNWORBC, SPOKRRJC, SPOKRRTC).	29
Figure 13. North Fork Rivanna River site photo.	31
Figure 14. Average and median streamflow calculated over the period 1993–2020 for the North Fork Rivanna River USGS Gauge 02032640.	32

Figure 15. Streamflow standard deviation calculated over the period 1993–2020 for the North Fork Rivanna River USGS gauge 02032640.....	33
Figure 16. HEC-RAS model geometry for Rivanna River flow model. The survey points are shown as black points, and linear features represent the cross sections (green line), centerline (dark blue line), bank lines (red line), and flow lines (cyan line).	34
Figure 17. Elevation of OHWM for XS1 at North Fork Rivanna River, VA.	35
Figure 18. Location and elevation of potential indicators of OHW on surveyed cross section a-a' across the North Fork Rivanna River, VA. The shaded blue area in the cross section represents the water surface (denoted by an inverted blue triangle) during the day of the survey and is not indicative of high flow.	35
Figure 19. Flood frequency curves based on AM and POT approaches for North Fork Rivanna River at USGS gage 02032640.	36
Figure 20. Rivanna River Cross Section 1 showing transition points for vegetation (top) and sediment (bottom). The water surface is the water surface during the day of the survey and is not indicative of high flow.	38
Figure 21. Regional OHWM flood frequency return period boxplot. Outliers removed from Table 4 have been eliminated.	42
Figure 22. Discharge relationship between field-delineated OHWM and bankfull elevations. Each data point represents a field surveyed cross section and is color coded based on geographic region.	43

Tables

Table 1. OHWM site locations, site codes for sites located on Figure 4 and survey dates.	27
Table 2. North Fork Rivanna River, VA, watershed characteristics.	31
Table 3. Return periods of the field identified OHWM indicators at Rivanna River Cross Section 1.	37
Table 4. POT and AM return period of OHWM. Outliers indicated by asterisk.	40

Preface

This study was conducted for the US Army Corps of Engineers (USACE) Headquarters through the Wetlands Regulatory Assistance Program (WRAP) under Funding Account Code U4375873; AMSCO Code o88893. The Program Manager was Mr. Kyle Gordon.

The work was performed by the Terrain and Ice Engineering Group of the Remote Sensing/GIS Center of Expertise, US Army Engineer Research and Development Center, Cold Regions Research and Engineering Laboratory (ERDC-CRREL). At the time of publication of this report, Dr. Meghan Quinn was team lead; Mr. David Finnegan was Division Chief. Dr. Jennifer M. Seiter-Moser is the Acting Technical Director for Civil Works Environmental Engineering and Sciences. The Deputy Director of ERDC-CRREL was Dr. David Ringelberg, and the Director was Dr. Joseph L. Corriveau.

COL Teresa A. Schlosser was Commander of ERDC, and the Director was Dr. David W. Pittman.

1 Introduction

1.1 Background

Streamflow influences the longitudinal and vertical distribution of high water marks (HWM) in a landscape. Streamflow, or discharge, is the volume of water moving through a stream channel per unit time and is described in units of cubic meters per second or cubic feet per second. Examples of HWMs are sediment deposits, changes in character and distribution of soil and vegetation, large wood accumulations, and other depositional and erosional features at elevations corresponding with high water (Wohl et al. 2016). In the absence of wetlands, the regulatory boundaries of the waters of the United States are delineated using HWMs that indicate *ordinary* high water levels. Ordinary high water mark (OHWM) is defined in 33 CFR 328.3(c)(7) as a “line on the shore established by the fluctuations of water and indicated by physical characteristics such as a clear, natural line impressed on the bank, shelving, changes in the character of soil, destruction of terrestrial vegetation, the presence of litter and debris, or other appropriate means that consider the characteristics of the surrounding areas.”

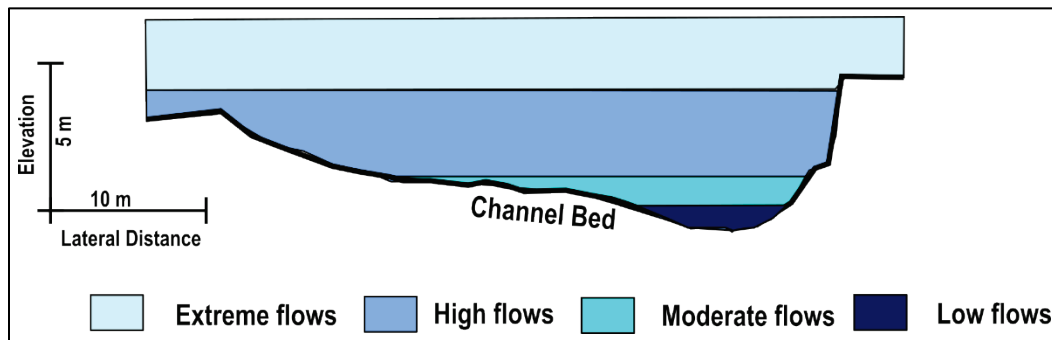
While OHWM defines the lateral extent of water boundaries of streams and rivers, the definition lacks any reference to the relationship between streamflow and the OHWM. USACE (2005) is the first regulatory guidance that mentions streamflow as a physical indicator of OHWM, but the guidance does not describe how streamflow can be used to define portions of a river channel that are more likely to support OHWM delineation (Lichvar et al. 2006). Streamflow is a fundamental control of river form and processes that are inherently related to climate, geology, topography, soils, and vegetation of the upslope landscape (Poff et al. 1997). The definition for OHWM describes HWMs that can be left by both common and extreme flooding events, which can create confusion when delineating the OHWM in certain landscapes (Mersel and Lichvar 2014). A detailed study of how the distribution of OHWM physical indicators relates to streamflow metrics can reduce uncertainty associated with delineating OHWM in diverse landscapes.

The relationship between streamflow and the concept of OHWM requires an understanding of the ecologic, hydrologic, and geomorphic flow

classifications that, at times, present confusing nomenclature. The difference in flow nomenclature arises because flows with ecological importance (i.e., habitat maintenance) occur in the lower-middle end of the flow spectrum (Beechie et al. 2012). In contrast, flows with geomorphic importance (i.e., channel forming flows) are the middle-higher end of the flow spectrum (Wolman and Miller 1960). Furthermore, hydrologic classifications tend to focus on describing flows based on frequency or probability of occurrence and not necessarily relate that to how the flows are significant for ecologic and geomorphic function.

Flows in the lower-middle end of the flow spectrum can be classified, relative to the smallest amount of water, into low, moderate, high, and extreme categories (Figure 1). Low flows correspond to the amount of streamflow that is most commonly observed in a channel. The moderate flow category exists to separate low flows from high flows. High flows correspond to flows that extend up to the top of river embankments and is the range in which the water surface elevation (OHW) of the OHWM is found. Flows that overtop the river embankments are considered extreme relative to low flows.

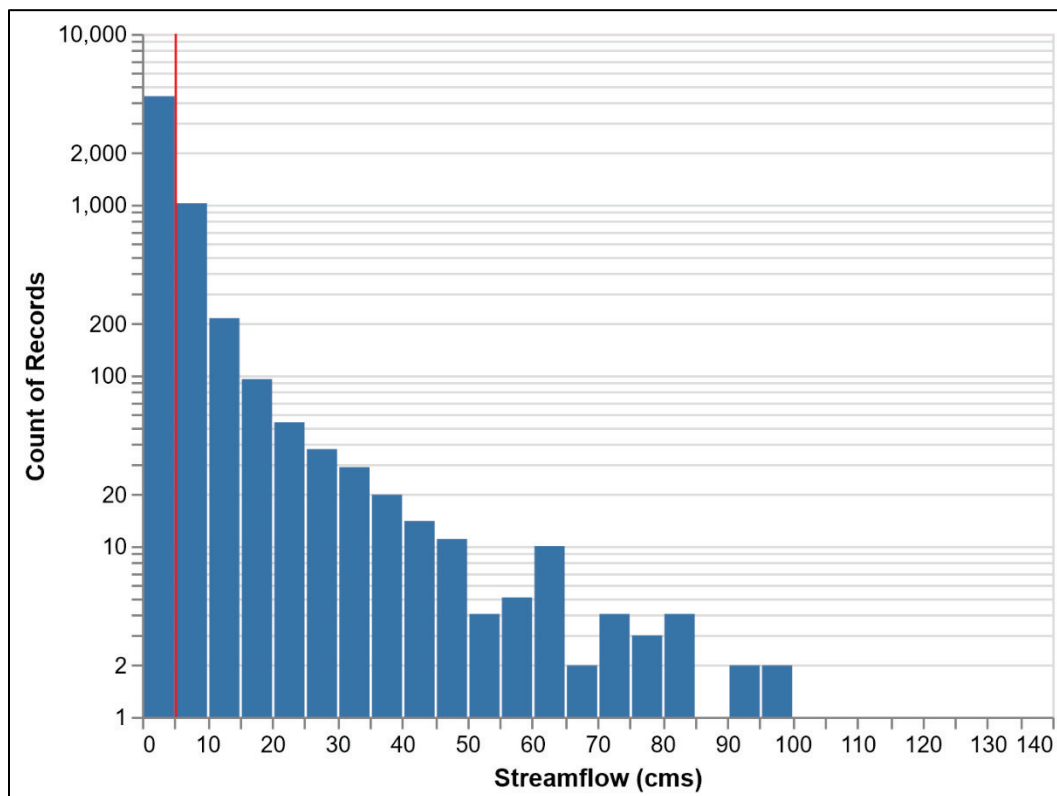
Figure 1. Conceptual diagram of flow classifications based on divisions that are of geomorphic and ecologic importance for a hypothetical cross section. The exact elevations bounding each flow category will vary based on channel type and various physical and vegetative indicators.



Classifying flows on the lower-middle and middle-upper ends of the flow spectrum also complicates how to compare statistical metrics between them because streamflow data are positively skewed (i.e., heavy right tail) by large-infrequent flooding events (Figure 2). For example, mean annual flow (MAF) (indicated by the vertical red line in Figure 2) occurs at a frequency of order of magnitudes more often than the largest observed flooding event. MAF corresponds to low flow category in Figure 1. To overcome this limitation of descriptive statistics, nonparametric statistics

and flood frequency are commonly used to describe the medium-upper end of the flow spectrum (Helsel et al. 2020). The middle-upper flows are also described by the high and extreme flows categories in Figure 1.

Figure 2. Bar graph of daily average streamflow record. The vertical red line shows the central tendency of the daily average streamflow record.

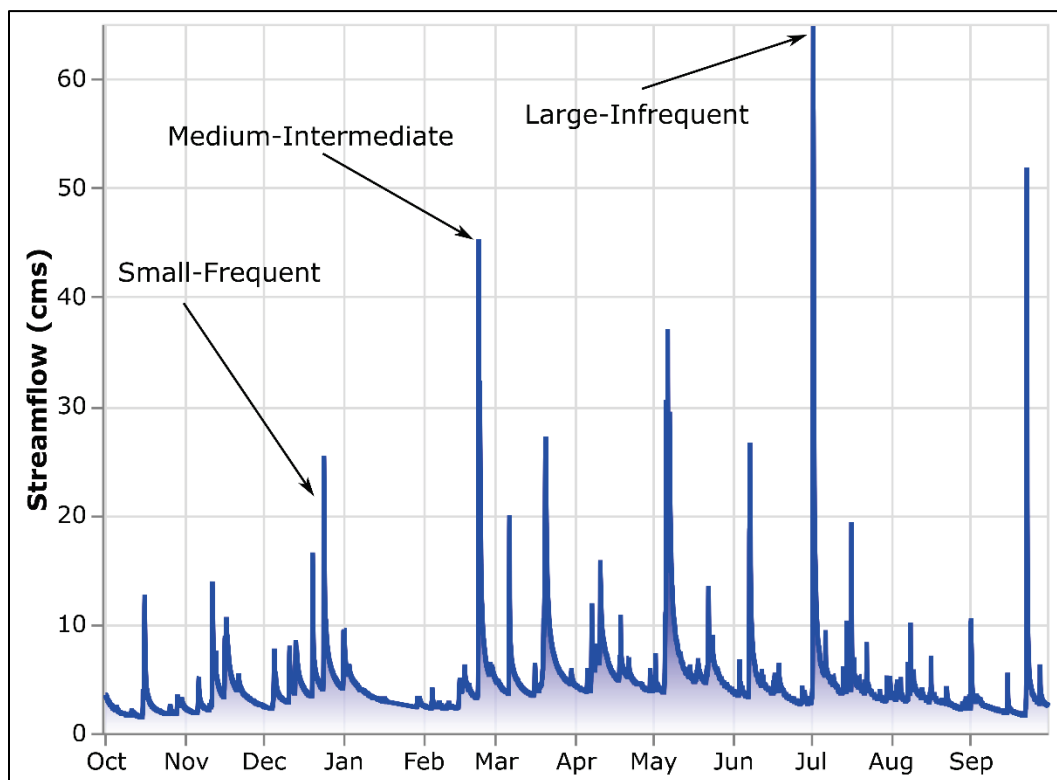


Flows in the middle-upper end of the flow spectrum are typically classified based upon magnitude and frequency relative to the largest out-of-bank flooding event (Oden and Poff 2003). Figure 3 depicts an example hydrograph where small-frequent, medium-intermediate, and large-infrequent events are labeled. The three magnitude-frequency categories represent the following:

- Small-frequent: small floods, often contained within a stream's banks, with little to no interactions with a floodplain.
- Medium-intermediate: medium floods, occasionally out-of-bank, will be contained within the active floodplain.
- Large-rare: large floods, typically always out-of-bank, can inundate areas beyond the active floodplain.

These magnitude-frequency categories are not the same that are identified based on geomorphic and ecologic attributes in a channel (Figure 1) because they consider temporal component of streamflow. Nonetheless, the bounding magnitude-frequency flooding categories can be attributed to specific geomorphic functions. Large-rare floods are responsible for floodplain formation and large wood recruitment (Wolman and Leopold 1957; Junk et al. 1989; Nanson and Croke 1992; Roni and Beechie 2013). Small-frequent floods are responsible for the shape of the channel, habitat formation, and sediment transport (Wolman and Leopold 1957; Wolman and Miller 1960; Andrews 1986). Based on these flow categories, small-frequent floods correspond to high flows in Figure 1 and are most likely related to OHW. Medium-intermediate and large-infrequent floods are described by extreme flows in Figure 1.

Figure 3. Labeled hydrograph identifying examples of flow events fitting within magnitude and frequency categories. Amounts of streamflow are described by the first term and the relative frequency.



The development of scientific concepts relate stream channel form to streamflow is a body of research that began in the 1950s (e.g., Leopold and Maddock 1953), largely after rivers were commonly instrumented with streamgages, and was not available to the original authors who defined

OHWL in the Rivers and Harbors Act of 1899. *Bankfull discharge* is the streamflow magnitude associated with a constant water level where a hydraulic transition between channelized (i.e., longitudinal) to lateral flow onto the floodplain occurs. The bankfull stage was initially defined as the vertical boundary between the active channel and surrounding floodplain (Wolman and Leopold 1957). *Stage* refers to the elevation of the water surface, usually above some arbitrary datum. Despite the fact that OHWM was defined for regulatory purposes and bankfull was defined as a scientific concept, there are many similarities between the definitions. The original definition of bankfull discharge and OHWM is similar in that they are general descriptions of vertical elevation thresholds where physical and vegetative transitions will occur. The following list summarizes the similarities between the two concepts by comparing the definition of OHWM to scientific descriptions of bankfull:

- “[a] clear, natural line impressed on the bank, shelving” – The boundary between the active channel and floodplain commonly exists as a clear, natural line impressed on the bank of a river (Wolman and Leopold 1957).
- “...changes in the character of soil” – The boundary between the active channel and surrounding floodplain creates hydraulic conditions that will cause a transition between river sediment and soils on an adjacent floodplain (Leopold and Skibitzke 1967).
- “...destruction of terrestrial vegetation” - Terrestrial vegetation is commonly destroyed by the hydraulic forces associated with flow below bankfull discharge (Leopold and Skibitzke 1967).
- “...the presence of litter and debris” – Litter and debris will likely be present or deposited above bankfull discharge (Leopold and Skibitzke 1967; Junk et al. 1989).

The similarity between the definitions of bankfull and OHWM begin to diverge in scientific literature because the concept of bankfull discharge has evolved from a simple delineation of a vertical elevation threshold into a statistical metric that is more closely related to streamflow than site morphology (Johnson and Heil 1996). The purpose and need to relate bankfull to discharge and specific flood frequencies is different than what is needed when identifying the OHWM, which can create confusion in the differing scientific applications of the terminology. For instance, Wolman and Miller (1960) questioned why stream channels are not large enough to carry the maximum flood that occurs in the region. Additionally, when

considering the most common low flows, why were channels larger than the base flows that occur in the channel throughout the year? They concluded that low flows are ineffective and do not contribute to channel shape whereas extreme flood flows are highly effective at moving sediment but do not occur often enough to control channel characteristics. Therefore, they concluded that the stream channel is the size of the bankfull channel because high flows occur frequently enough to control the channel size, meaning that high flows are the dominant channel-forming discharge in alluvial streams. Understanding the flows that are most responsible for shaping the channel is useful for determining channel dimensions needed in channel restoration, computing sediment loads and budgets, and ultimately for a common reference to compare sites and develop regional curves. Although the ultimate purposes in applying the definitions are different, the overlap in the scientific concept of bankfull and the regulatory definition of OHWM allows an exploration of the connections between them and the underlying relationship with streamflow.

The most common statistical metric to describe bankfull is a return period, which describes the probability a flow will occur within a block maxima. A return period is estimated from an analysis of the magnitude and frequency of flooding events derived from a systematic record of streamflow. While a flood frequency analysis combines two of the hydrological indices (i.e., magnitude and frequency), the added complexity introduces uncertainty that muddles the original definition of bankfull discharge from a deterministic vertical elevation, to discharge associated with a return period of fewer than 2 yr¹ on perennial alluvial rivers (Leopold et al. 1964; Castro and Jackson 2001). Alluvial rivers are rivers that control their channel shape based on the amount of water and sediment that is moving through the system. The shape of bedrock streams is more likely to be controlled by cataclysmic events, which may make it difficult to identify a bankfull elevation. Furthermore, since bankfull flows are not responsible for forming these bedrock streams, it may not always be a useful concept to apply to these channels. In rivers where bankfull elevation is not easily observed, the range of return periods associated

¹ For a full list of the spelled-out forms of the units of measure used in this document, please refer to *US Government Publishing Office Style Manual*, 31st ed. (Washington, DC: US Government Publishing Office 2016), 248-52, <https://www.govinfo.gov/content/pkg/GPO-STYLEMANUAL-2016/pdf/GPO-STYLEMANUAL-2016.pdf>.

with bankfull discharge can become larger than 2 yr. Williams (1978) found bankfull discharge can be related to return period up to 32 yr in a national study. Arid systems can be particularly complex because channel shapes are sometimes controlled by larger flood events, mainly because all flow events are so infrequent that these systems may not have had time to respond and return to pre-flood conditions (Brunsden and Thornes 1979). However, what could be considered an ordinary high flow in a system like this would be very different than an ordinary high flow in a perennial alluvial system (Lichvar and Wakeley 2004; Lichvar and McColley 2008; Mersel and Lichvar 2014; Gartner et al. 2016a; Gartner et al. 2016b).

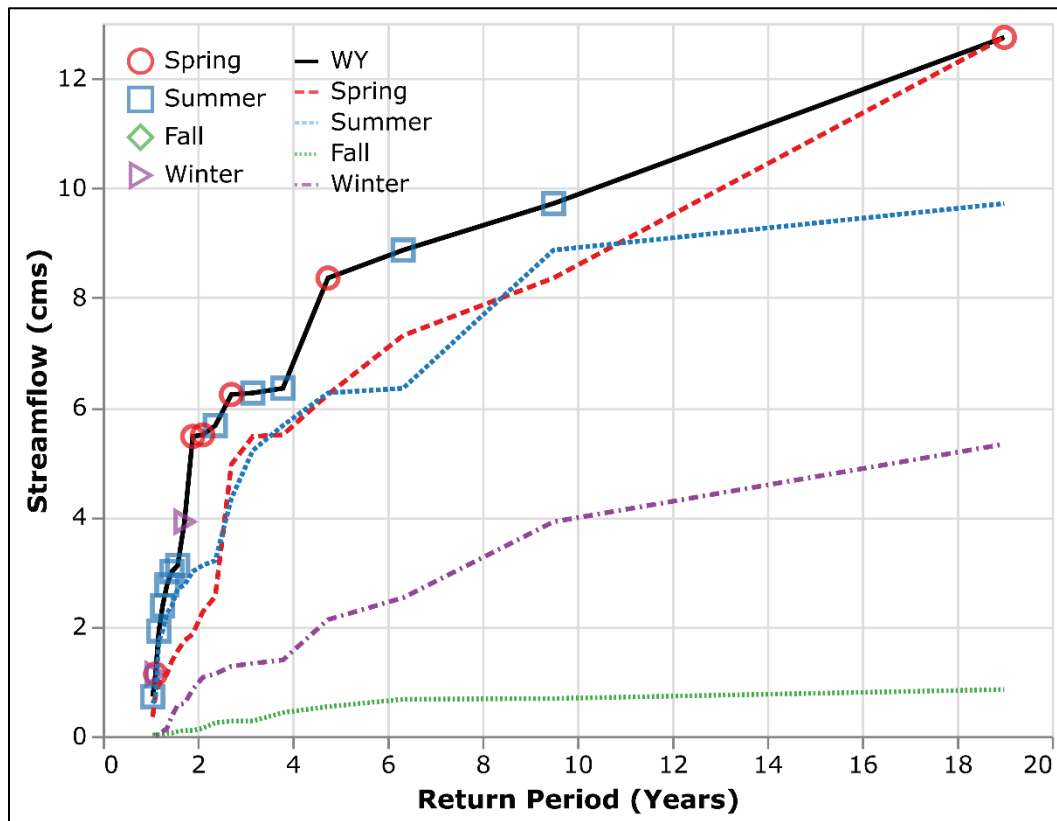
The precision of streamflow metrics derived from flood frequency analysis is influenced by the availability of streamflow data. Streamflow data are limited to instrumented river reaches, and the length of the record varies between streamgages. The sparse nature of streamflow data introduces uncertainty into flood frequency analysis because making direct comparisons between streamgages requires a record sufficiently long to capture the natural variability of the hydrologic regime. In different climates, the criteria of *sufficiently long* will vary. When streamflow records do not capture the natural variability, regional flood frequency methods can be used to characterize streamflow (Sherwood and Hytger 2005; Krstolic 2007). Regional methods rely on a regression analysis of streamgage and topographic data from a larger region. The use of multiple streamgages creates a streamflow record with an effective length that is suitable for flood frequency analysis. Regional flood frequency analysis will help provide context for the general behavior of streamflow in a particular region but introduce spatial and temporal uncertainty into the metrics (Harkins and Green 1981).

A relationship between OHWM and return period is complicated by the fact that accepted guidelines (e.g., Casterllarin et al. 2012; England et al. 2019) for performing flood frequency analysis are largely used to quantify return intervals with extremely rare events (Coles 2001). Previous OHWM literature (Bradley and Simons 1990; Lichvar and McColley 2008; Mersel and Lichvar 2014; Gartner et al. 2016a; Gartner et al. 2016b) acknowledges return periods could be used to describe individual discharges that relate to OHWM but cautioned against interpreting return periods as a quantitative metric that can be used to relate streamflow and OHWM nationally. Similar to the discussion about the relationship between bankfull discharge and return periods, regional and sub-regional

variation of OHWM will also present challenges in assigning a single return period to OHWM (Wohl et al. 2016). For example, Curtis et al. (2011) analyzed several sites in the arid Southwest and found OHWM was related to return periods up to 15 yr. There is a general consensus that OHWM on a national basis is associated with streamflow with return periods ranging from 1 to 10 yr (Wohl et al. 2016). The significance of a 10 yr range of return period implies OHWM is related to small-frequent and medium-intermediate flooding categories in Figure 2.

Quantitative relationships between flood frequency and OHWM are difficult to ascertain because the time interval that a flood frequency analysis is based on has a profound impact on describing flooding events that are related to the OHWM elevation. Longer time intervals will bias the analysis towards the most extreme flooding events, which are not related to OHWM. Smaller time intervals will result in a sample of flooding events that are more closely related to OHWM but might violate the theoretical basis for flood frequency. Figure 4 shows how seasonal or annual sampling of a streamflow record influences discharge estimates for different return periods. The sample of data representing a water year (WY) (October 1 – September 30) relates shorter return periods to larger amounts of streamflow. The annual sampling curve is related to seasonal flooding events from the spring (N=6), summer (N=11), and winter (N=2) seasons. In this example, fall flooding events are smaller than the other seasons and did not contribute to the annual sampling of events. A sample of flooding events that occur in different seasons could represent events from multiple flooding mechanisms (e.g., snowmelt, extended periods of precipitation, urbanized floods). An implication of the annual sampling strategy is there is a large range of streamflow that correspond to similar return levels. For example, return periods ranging from 1 to 2 yr correspond to streamflow ranging spanning an order of magnitude (0.5 to 5.5 cms).

Figure 4. Annual maximum return periods calculated for individual seasons and WYs. The return periods were calculated using the Weibull plotting position formula (return interval = $[N+1]/m$, where N is the number of years in streamflow record and m is the rank of each discharge value from largest to smallest). The color dots on the WY curve indicate which season the flooding event occurred.



1.2 Objectives

There are three main objectives of this study:

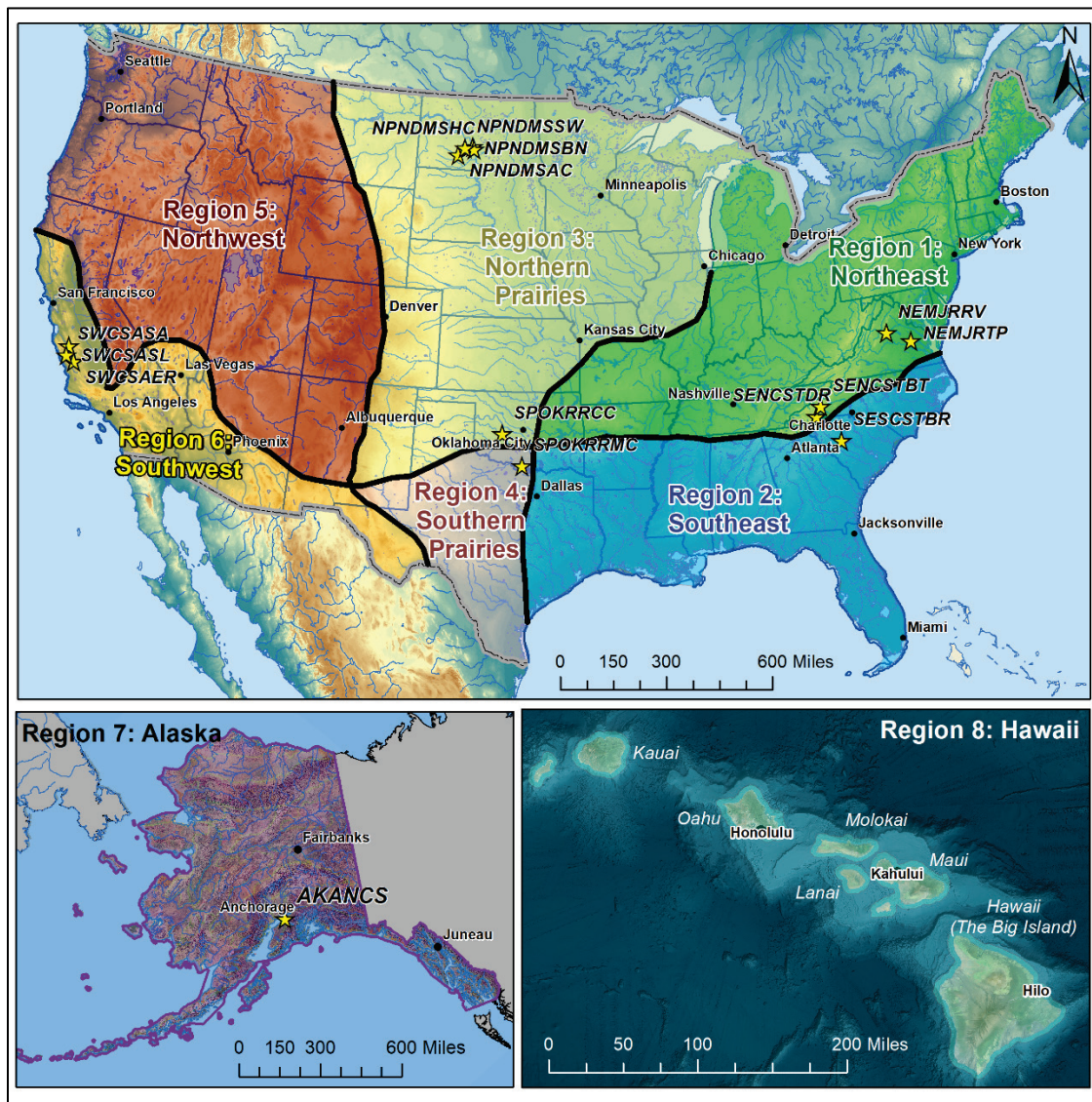
- Investigate the regional difference between OHWM indicators and streamflow.
- Evaluate flood frequency-return periods that describe flow related to OHWM elevation.
- Provide guidelines on the appropriateness of flood frequency analysis to support OHWM delineations.

1.3 Approach

Our approach to investigating the relationship between magnitude-frequency streamflow metrics and physical indicators of OHWM is based on a dataset of field surveys collected in the continental United States and Alaska (Figure 5), which are representative of the six of the eight

geographic regions identified in Wohl et al. (2016). The field dataset was collected in support of the development of a national manual that describes the OHWM delineation process. The field surveys consisted of topographic measurements of multiple cross sections and OHWM indicators at sites with established US Geological Survey (USGS) streamgages.

Figure 5. National map showing the country divided into 8 geographic regions and 15 study sites (yellow stars with eight-letter site code) distributed across six of those regions.



To provide insight as to whether frequency-magnitude streamflow metrics derived from flood frequency analysis can be used to identify and delineate OHWM, we evaluated two methods for calculating flood frequency. First,

we evaluated a traditional annual maximum (AM) approach following guidance in Bulletin 17C (England et al. 2019), hereafter referred to as Bulletin 17C. Second, we evaluated a less common partial duration series using peaks-over-threshold (POT) sampling. The formulations of each flood frequency approach are described in Section 2. The primary motivation for considering both flood frequency techniques is because traditional formulations, like Bulletin 17C, emphasize extrapolating beyond the largest observed flooding events, which are larger than the expected range of flows to relate to OHWM.

One-dimensional, steady state Hydrologic Engineering Center River Analysis Software (HEC-RAS) (USACE 2016) hydraulic models were developed to calculate water surface elevations of magnitude-frequency flood frequency metrics. The methodology used to develop the hydraulic models is described in Section 3. A case study is presented in Section 5 to demonstrate how constant level streamflow representations can be used to relate magnitude-frequency streamflow metrics and OHWM indicators. Finally, the study results are aggregated to explore the applicability and regional differences of return periods related to OHWMs (Section 5.2 and 5.3).

2 Flood Frequency

Flood frequency analysis is used to statistically quantify probabilities of different-sized flooding events using a sample of observed flooding events. The results of a flood frequency analysis are used to estimate the probability that a flooding event will occur on a specified time period. For large-infrequent events (lower probability), these flooding probabilities are used to define the economic and life risks associated with infrastructure within and adjacent to the river floodplain. For small-frequent events (higher probability), the flooding probabilities have been used to describe bankfull discharge (Wohl et al. 2016). The OHWM elevation likely corresponds with the streamflow elevation of these higher probability events; therefore, partial-duration series flood frequency approach is explored in this study to better understand if it is an improved way to quantify flood frequency for these smaller magnitude floods.

Flood frequency analysis is based on the theory of extreme values. The main objective of any extreme value analysis is to quantify the stochastic behavior of a process when the exact statistical behavior is unknown (Coles 2001). In flood frequency applications, the process is streamflow, and the unknown behavior is future flooding events. To perform a frequency analysis of extreme flooding events, a block maxima sample (M_n) of peaks from flooding events (X) over an n -length observation period needs to be extracted from a systematic record of streamflow (Equation 1).

$$M_n = \max\{X_1, \dots, X_n\} \quad (1)$$

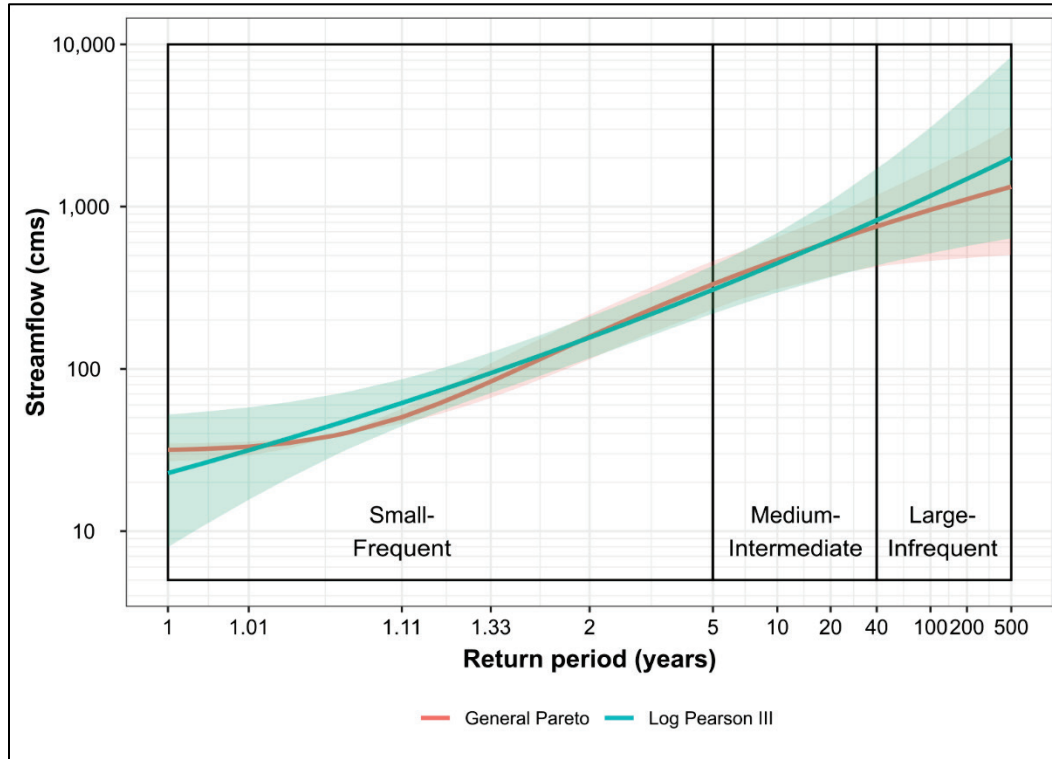
Sampling strategies are selected such that there is hydrological independence between successive flooding events, and the overall behavior of the streamflow record does not show long-term increasing or decreasing trends. Bulletin 17C recommends using an AM approach that requires sampling instantaneous streamflow records (i.e., 15 min) using a block maxima filter with a block length of one WY. Instantaneous streamflow records (i.e., 15 min) are the most suitable for flood frequency analysis because average daily streamflow records are not representative of quick-moving flooding events. For example, flooding event peaks typically occur at a sub-hourly time-step, and average daily discharge is averaged across the rising and falling limb of flooding hydrographs. Bulletin 17C cautions average daily streamflow for flood frequency if the

peak streamflow record is shorter than 10 yr and can only be used to quantify short (e.g., < 15 yr) return periods. In this case, an annual block maxima filter would likely result in a systematic underrepresentation of magnitude-frequency estimates of large (e.g., > 15 yr) return periods. To overcome the under-representation of flood magnitude associated with flood frequency analysis using average daily streamflow, Bulletin 17C suggests using a partial duration flood frequency analysis using a POT sampling technique. In this report, we will use POT to refer to partial-duration flood frequency analysis using a POT sampling technique.

The primary source for recommendations and guidelines for partial-duration flood frequency analysis using POT sampling is found in scientific literature (Langbein 1949; Madsen et al. 1997; Claps and Laio 2003). A primary difference between Bulletin 17C and POT flood frequency analysis is the choice of statistical distribution. Bulletin 17C recommends using a Log Pearson III (LP3) while POT uses a General Pareto (GP) distribution (Figure 6). Although the LP3 and GP have different formulations, they produce similar flood frequency curves, with subtle differences at the tails of the distributions. The uncertainty of the lower tail (i.e., small-frequent) of the GP distribution is less than the LP3 because GP distribution has less curvature.

The underlying methodology for the AM and POT flood frequency is described in Section 2.1 and 2.2. AM is the most common approach develop magnitude-frequency relationships but is primarily designed to extrapolate beyond the largest observed events (i.e., above OHW). POT is explored because there is a potential quantifying magnitude-frequency relationship that better describes variability small-frequent flooding events. These two methods were applied to the USGS streamgage data at every site and used to determine magnitude-frequency for flows found at the elevation of the OHWM.

Figure 6. Example showing differences between GP and LP3 statistical distributions for flood frequency analysis. The approximate thresholds for small-frequent, medium-intermediate, and large-infrequent flooding events are shown using rectangles with black outlines. The uncertainty bounds for each distribution are shown by the shaded regions.



2.1 Annual maximum (AM)

Bulletin 17C recommends flood frequency analysis using AM approach. The sample of flooding events used to calculate magnitude-frequency relationships is sampled using an annual block maxima filter applied to a record of instantaneous streamflow. Block lengths less than one WY can be selected, but the assumption of hydrological independence requires a time-step sufficiently large to ensure the distribution of peak discharge remains random. Bulletin 17C recommends fitting the sample of flooding event to an LP3 distribution. The cumulative distribution of an LP3 is defined in Equation 2.

$$F(x) = \frac{\alpha^k (y - \varepsilon)^{k-1} e^{-\alpha(y - \varepsilon)}}{x \Gamma(k)} \quad (2)$$

Where α is the scale, k is the shape parameter, y is the log-transformed streamflow X , and ε is the location parameter. The LP3 distribution

parameters are estimated from the sample moments mean (μ), standard deviation (σ), and skewness (γ).

$$\alpha = \frac{\sigma_y}{k}$$

$$k = \frac{4}{\gamma_y^2}$$

$$\varepsilon = \mu_y - \sigma_y \sqrt{\beta}$$

The N -year return level is a function that is calculated using Equation 3.

$$y_N = \mu_y + K_N \sigma_y \quad (3)$$

Where K_N is a frequency factor, μ_y and σ_y are the mean and standard deviation of the population of log-transformed streamflow y , respectively. K_N is a tabulated value, that relates γ to exceedance probabilities, because the cumulative distribution for LP3 cannot be inverted to directly calculate y_N (Stedinger et al. 1993).

2.2 Peaks-over threshold (POT)

The underlying principle of the POT method is that extreme flooding events suitable for flood frequency analysis do not occur on a regular time step (Langbein 1949, Langousis et al. 2018). POT flood frequency is also commonly referred to as partial duration, where “partial” indicates the flood event only describes a portion of a WY. In an abnormally dry year, the largest flooding event could be smaller than more common flows during wet years. Conversely, an abnormally wet year could have multiple extreme flooding events. Distributions of flooding events are generated by providing a minimum flood magnitude and/or a minimum amount of time between peaks. A common distribution used for extreme values is the GP distribution with the cumulative distribution function defined in Equation 4.

$$F(x) = 1 - k \left(\frac{x-u}{\alpha} \right)^{1/k} \quad (4)$$

Where k is the shape parameter, α is the scale parameter, x is a peak streamflow, u is a threshold. GP is the most common statistical

distribution for POT frequency analysis because the threshold can be directly parametrized in the distribution. When $k = 0$, the GP reduces to an exponential distribution. When using peak flow records, k values range from -0.9 to 0.5. When $k < 0$, the distribution has a heavy right tail and does not have an upper bound and assumes a convex shape. When $k > 0$, the GP has an upper bound of $u - \frac{\alpha}{k}$ and has a concave shape. The m -observation return level (x_m) is a function of the distribution parameters from the GP and using Equation 5.

$$x_m = u + \frac{\alpha}{k} [(m\zeta_u)^k - 1] \quad (5)$$

Where m is the return level, ζ_u is the probability of a peak discharge exceeding threshold u . x_m can be modified to calculate annual return periods by accounting for how many discharge values fall within the same year (Equation 6).

$$x_N = u + \frac{\alpha}{k} [(Nn_y\zeta_u)^k - 1] \quad (6)$$

Where N represents the annual return period and n_y is the average number of events each year.

The process of finding an appropriate threshold level is a critical step for a POT flood frequency that has limited widespread application in flooding studies. If the threshold is too low, then the events will not have hydrological independence and the flood-frequency analysis will be invalid because the sample includes too many within-bank flooding events. If the threshold is too high, then there would not be enough events to properly fit a GP distribution. Because the OHWM is likely related to small-frequent flood events, we were interested in investigating a method that allows more of these events into the analysis. There are tests, called goodness of fit (GOF), to assist in determining a threshold in an unbiased way. Methods for deciding an appropriate threshold can be completed using graphical or GOF tests (Coles 2001). Graphical methods (e.g., mean residual plot, hill diagrams) are semi-quantitative in selecting thresholds as they rely on a user's judgment of parameter stability. A quantitative alternative to graphical methods is GOF tests. GOF tests are performed to ensure the candidate threshold yields a sample of independent flooding events and is adequately represented by the GP distribution.

2.2.1 Goodness-of-fit (GOF)

In this study, we used an analytical approach to select an appropriate threshold for POT-based flood frequency informed by GOF tests. In general, GOF tests are designed to be performed in a sequential order to determine if any of the underlying assumptions of flood frequency are violated. When a distribution of flooding events passes all of the GOF tests at a specified confidence level, the distribution can be deemed valid. The process for a sequence of thresholds yields a set of candidate thresholds that do pass the GOF tests at a provided confidence level. Mann-Kendall and Cramer-von Mises are the two GOF tests used to ensure hydrological independence exists between the distribution of peaks and to verify the data follow a GP distribution, respectively.

2.2.1.1 Mann-Kendall

The non-parametric Mann-Kendall test statistic was used to determine if a distribution of floods had any trends in time. When monotonic trends are present in a daily flow time series, the assumption of hydrologic independence between peak values is likely invalid. A monotonic trend in a POT sample of flooding events could indicate that the events are not hydrologically independent and a higher threshold would be more appropriate. Across the period of record, a monotonic trend could indicate nonstationarity, where the central tendency changes across the time series. For an n -length sequence of peak flows M_n , the Mann-Kendall statistic checks the later and earlier peaks for an increasing or decreasing trend. Mann-Kendall tau statistic (τ) is defined in Equation 7.

$$\tau = 1 - \frac{4N_d}{(N-1)(N-2)} \quad (7)$$

where N_d is the number of disordinate pairs and N is the sample size. The τ statistic ranges from -1 when a decreasing trend is present and +1 with an increasing trend. When the $|\tau|$ is close to zero, the test fails to reject the null hypothesis, meaning there is not enough data to conclude there is a monotonic trend in the data. In this report, we used a significance level ($\alpha = 0.05$) to make all interpretations using the τ statistic.

2.2.1.2 Cramer-von Mises

The Cramer-von Mises is a test to determine how well a sample of peak discharge values are described by a GP distribution. The test is a measure

of the square displacement between an empirical and theoretical distribution with the same distribution fitting parameters. For a GP distribution, Choulakian and Stevens (2001) have published acceptance levels for the Cramer-von Mises statistic (W^2) approximated using Equation 8.

$$W^2 = \sum_{i=1}^N \left(F(q_i) - \frac{(2i-1)}{2N} \right)^2 + \frac{1}{12N} \quad (8)$$

where

q_i = i-th order statistic of an empirical sample

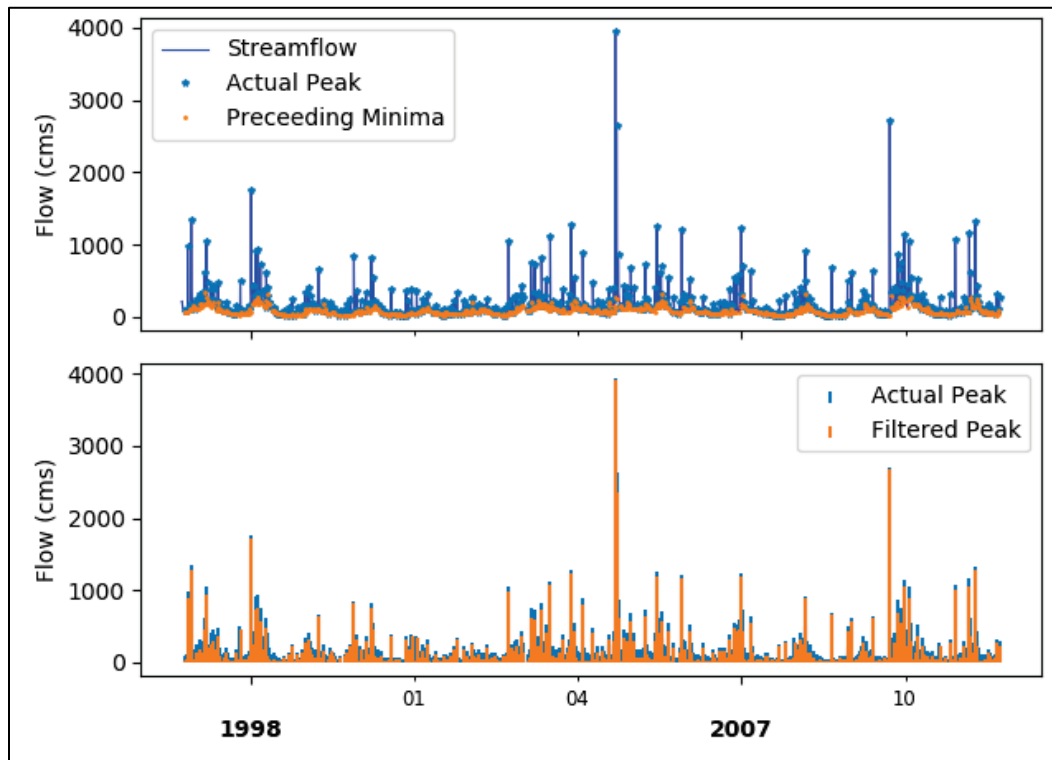
F = GP distribution

N = size of the empirical sample.

2.2.2 POT threshold selection

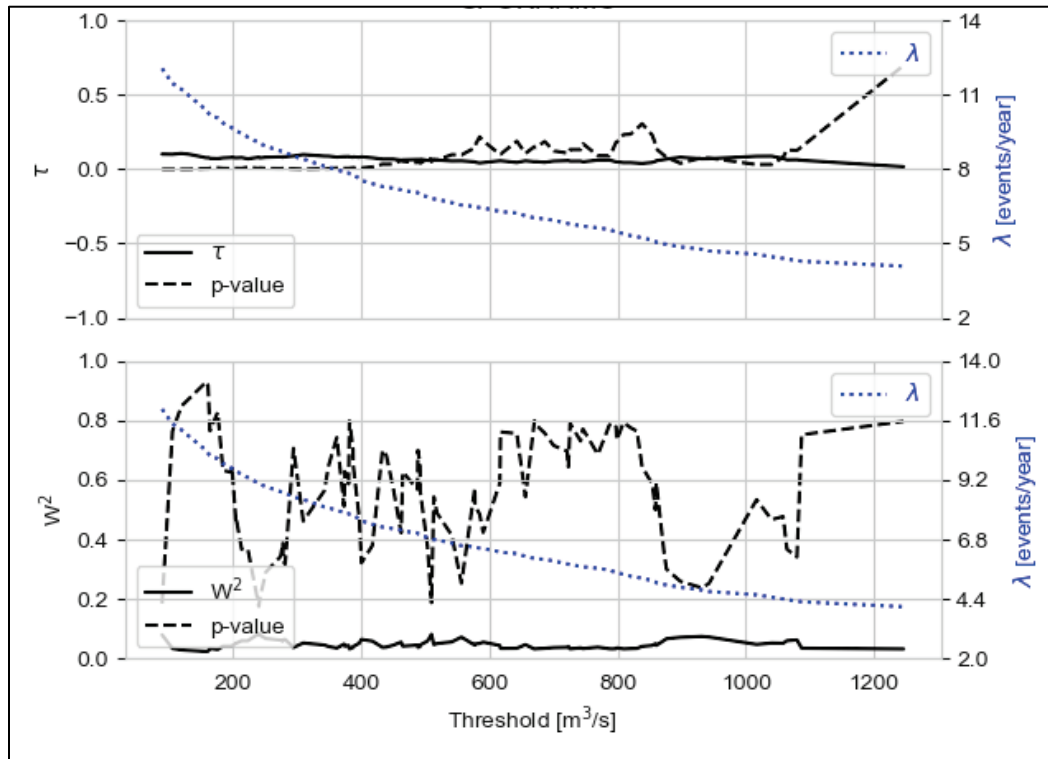
A POT threshold represents an appropriate streamflow threshold that results in a sample of flooding events suitable for flood frequency analysis from a daily average streamflow record. In this study, we used an analytical approach for POT threshold selections described in Claps and Laio (2003). The filtered peaks over threshold (FPOT) consists of deriving a sample of threshold candidates by filtering the population of peak discharges from a systematic record of average daily discharge. The population of daily discharge values is filtered by subtracting the preceding minima on the hydrograph from the subsequent peak value. In effect, this approach filters out peaks associated with base flow periods by allowing them to be filtered out with a very low FPOT threshold (Figure 7).

Figure 7. Example of the FPOT filtering. Top panes show the daily discharge record with peaks and preceding flood minima. The lower panel shows a comparison of the FPOT and actual magnitude of the overall flooding event.



In ascending order of filtered peaks, the threshold level associated with a filtered peak was used to fit a GP distribution. GOF tests were used to determine if a threshold produced a distribution of flooding events that were described by a GP distribution. Since the threshold being tested was identified using a filtered dataset, the threshold used to fit the GP distribution was set to the minimum from the candidate distribution (Figure 8).

Figure 8. Example showing how GOF tests were used to identify a set of thresholds that are well described by the GP distribution. A suitable threshold for this example would exist between 600 and 800 cms because the τ and W^2 are both less than the p-value.



2.3 Parameter estimation

The fitting parameters for a flood frequency distribution (Equation 2 and Equation 4) are estimated in a process called parameter estimation. Coles (2001) describes the parameter estimation methods used in flood frequency as two categories, (1) deterministic and (2) Bayesian. The distribution fitting parameters ($\theta = f(\alpha, \kappa)$) in a deterministic approach are considered constant, while the parameters are allowed to vary in Bayesian models. A major difference between the two approaches to parameter estimation is how uncertainty is calculated. For deterministic methods, confidence intervals can be assigned to individual quantiles relying on the asymptotic theory of probability distribution function (Coles 2001). In the Bayesian approach, uncertainty can be directly quantified using the variability in the resulting posterior distribution. All the flood frequency analyses performed in this study were completed in the R computing language (R Core Team 2020) using Rstudio (RStudio Team 2020).

For the AM flood frequency using the LP3 distribution, we used the deterministic method-of-moments for parameter estimation. The underlying principle of method-of-moments is that the statistical moments (i.e., mean, variance, skew, and kurtosis) of a sample of flood events are assumed to describe the population of all possible flood levels. This assumption allows for the probability of most extreme flooding events to be estimated using statistical inference. Confidence intervals were calculated using a bootstrap technique with 10,000 samples and a 10% significance level. In this study, all LP3 distributions were fitted using the “lmomoco” R package (Askquith 2020).

For the POT flood frequency using the GP distribution, we used a Bayesian method for parameter estimation. For this method, a posterior distribution of distribution parameters was determined using a Markov Chain Monte Carlo sampling technique (Gilleland and Katz 2016). The GP distributions were fit using the “extRemes” package. All GOF tests were performed using “eva” R package (Bader and Yan 2016).

3 Hydraulic Modeling Approach

Hydraulic models simulate the conveyance of water in steady (i.e., constant water elevation) or unsteady (i.e., water elevations that fluctuate over time) simulations. Steady simulations are commonly used in design calculations that do not require a detailed analysis of the temporal variation of streamflow. Steady simulations were used to characterize flows in this study to allow for direct comparison of a modeled OHW stage with field delineations of the OHWM (Gartner et al. 2016a).

3.1 Flow model formulation

The HEC-RAS was used to develop one-dimensional hydraulic models (USACE 2016). The hydraulic properties for a particular flow rate are calculated using equations that describe basic water profile properties (e.g., water surface elevation) and flow conveyance equations that account for frictional properties (e.g., forces exerted on the riverbed) of water conveying over a natural riverbed. Basic profile properties between two cross sections are calculated using the open channel for steady-state hydraulics form of the Bernoulli equation (Chow 1959; Einstein and Barbarossa 1952; Bjerklie et al. 2005):

$$Z_2 + Y_2 + \left(\frac{V^2 a}{2g}\right)_2 = Z_1 + Y_1 + \left(\frac{V^2 a}{2g}\right)_1 + h_e \quad (9)$$

where

- Z = water surface elevation (m)
- Y = depth of water (m)
- V = average water velocity (m/s)
- a = velocity weighting component (-)
- g = gravitational constant (m/s²)
- h_e = energy head loss (m).

The Z , Y , and $\left(\frac{V^2 a}{2g}\right)$ terms represent the elevation head, pressure head, and velocity head, respectively. The elevation head describes the potential energy of a volume of water moving from high to low elevation. The pressure head term describes the energy associated with the geostatic pressures in a water profile. Velocity head describes the energy associated with the kinematic motion of a water body over a natural riverbed. The last

term (h_e) is used to account for the losses associated with mechanical energy losses from viscous stresses.

The velocity head term in the energy balance is calculated using Manning's equation (Equation 10), which relates flow velocity with frictional losses associated with conveyance over a natural riverbed (Chow 1959; Einstein and Barbarossa 1952).

$$V = \frac{1}{n} R^{2/3} S^{1/2} \quad (10)$$

where

V = water velocity (m/s)

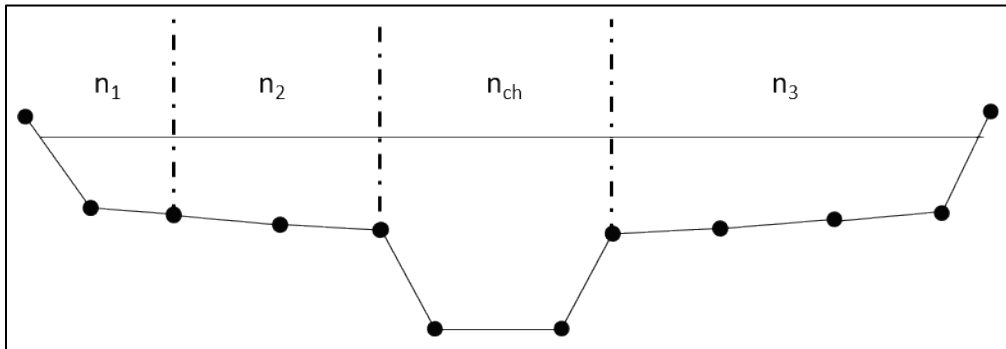
R = hydraulic Radius (m)

S = friction slope (-)

n = hydraulic roughness coefficient (Manning's coefficient)
(s/m^{1/3}).

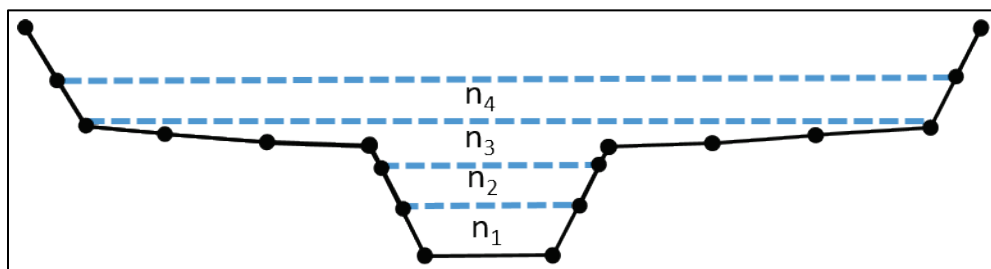
Hydraulic roughness varies based on flow, channel morphology, and submergence of roughness elements. The hydraulic roughness coefficient is a function of three physical components: (1) grain (e.g., viscous and pressure drag on grains), (2) form (e.g., pressure drag on bed and undulations), and (3) spill resistance (e.g., energy losses associated with water accelerating over a drop) (Einstein and Barbarossa 1952; David et al. 2011; Yochum et al. 2012). To account for the variations in hydraulic roughness, HEC-RAS allows for horizontal and vertical variation of the roughness coefficients. Horizontal variation of the roughness coefficient is the most common approach for modeling intermediate to large flows because the proportion of the water column interfacing with the riverbed becomes very small. An example diagram of horizontally varied n is shown in Figure 9. For a cross section divided into n -segments, the model calculates the conveyance of each segment using the specified roughness coefficient. Once all the calculations were made for individual segments, the resulting values are summed together to calculate total conveyance for a cross section. Horizontal variations in hydraulic roughness are required to accurately model the hydraulics occurring in the channel and floodplains. The most common approach is to divide the channel into three segments: (1) left flood plain, (2) in-channel, and (3) right flood plain. Each segment can be further divided if the cross section has complex bathymetry.

Figure 9. Example cross section showing the horizontal variation of Manning's roughness.



Vertical variation of the hydraulic roughness is desirable for low flow and high gradient (i.e., $S > 2\%$) streams (Figure 10). At low flows, hydraulic roughness increases non-linearly because the relative size of riverbed features to the depth of flow becomes large. High gradient streams also introduce additional complexities for hydraulic roughness calculations because the channels typically have a mixed flow regime consisting of supercritical and subcritical flows. Transitions between different flow regimes also introduce a spill resistance, where energy loss occurs as flow transitions from a steep drop to a lower gradient through a hydraulic jump. A major limitation to developing flow models calibrated using a vertical variation of hydraulic roughness is the model requires detailed, site-specific measurements of discharge and velocity that are not commonly available in ungauged streams. Most commonly, the vertical variation of hydraulic roughness is parameterized to get model simulations to match an empirical relationship between stage and discharge.

Figure 10. Example cross section showing the vertical variation of Manning roughness values.



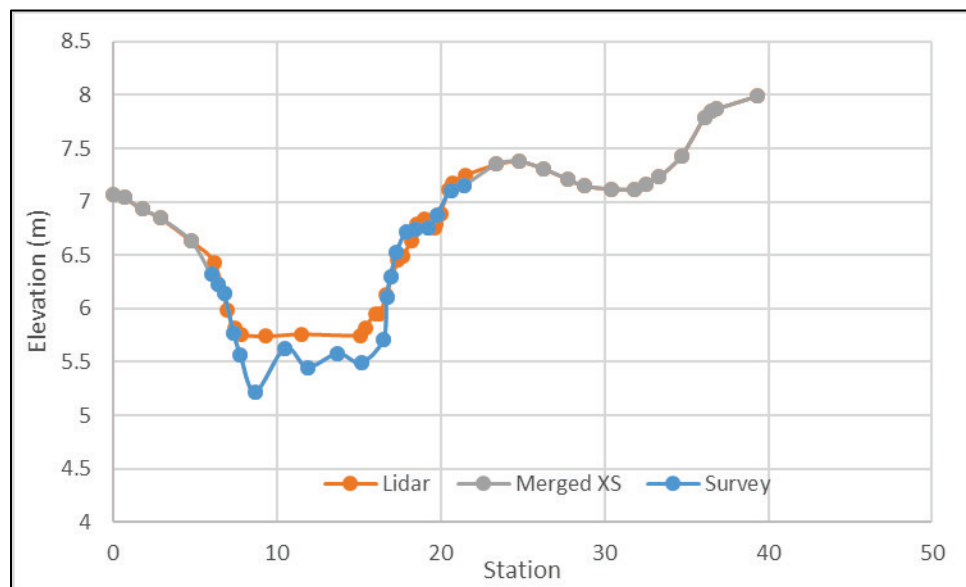
In this study, estimation of hydraulic roughness on low gradient streams (i.e., slopes $< 2\%$) relied on tabulated values for different grain size and morphological characteristics of a river (Barnes 1967; Yochum et al 2014.). In absence of calibration data (e.g., rating curve, historical flood

inundation levels, or previous models of the study reach), tabulated hydraulic roughness values are commonly used because the dominant component of hydraulic roughness is captured by relatively simple characteristics of riverbeds and floodplains.

3.2 Georeferencing

Georeferenced flow models were created using a combination of the Rasmapper application within the HEC-RAS 5.0.7 software package and geographic information systems (GIS). The survey points were post-processed in Trimble Business solutions survey software. The resulting point cloud was converted to a shapefile and assigned an appropriate Universal Transverse Mercator (UTM) projection. The survey point cloud was imported into Rasmapper and used to build an initial model geometry. The initial geometry consisted of a river centerline, bank lines, cross sections collocated with the survey points, and a terrain model created from a bare-earth digital elevation model (DEM) product. The DEMs were collected from a variety of GIS data portals, but an emphasis was placed on finding the highest resolution product, which typically came from state GIS resources. Bare earth DEM resolutions varied from 1 m to 30 m, with 30 m DEMs being from the USGS three-dimensional elevation program (formally the National Map) dataset. The Rasmapper application was then used to assign elevations from the terrain model to each cross section and calculate stationing information. The bathymetric information for the field survey was merged with the surrounding DEM in a Microsoft Excel spreadsheet. In the spreadsheet, any horizontal or vertical offsets were applied to merge the survey points with the floodplain topography (Figure 11). If a vertical offset was applied to the survey data, the same offset was applied to all of the surveyed points to ensure the relative positioning of the cross sections was preserved.

Figure 11. Example showing the merging process of survey points and collocated DEM derived cross section (XS).



The resulting geometry of bathymetric and floodplain topography was then used to create an interpolated bathymetric surface in Rasmapper. The interpolated cross-section algorithm was used to create a channel DEM between the bank lines from the original model geometry. This information can be merged with the original terrain model to create a composite surface that contains data from the field survey and surrounding flood plain topography.

3.3 Calibration

The flow models developed for this study were primarily calibrated using the hydraulic roughness coefficient. At sites where the surveyed cross sections were close to a streamflow gage and no major changes in channel shape exist, the models were calibrated to USGS rating curve. This was achieved by vertically and horizontally varying the hydraulic roughness to match the modeled and observed rating curves.

For low-gradient streams, the model was run using sub-critical flow with a normal depth boundary condition at the downstream cross section.

4 Data Sources

4.1 Field surveys

The OHWM sites were surveyed between the fall of 2016 through 2017 (Table 1). The surveys consisted of topographic surveys and detailed field observations across each of the identified geographic sub-regions for OHWM (Wohl et al. 2016). The basis behind the delineation of six geographical continental United States regions is to capture the variations in vegetation that occur across the eastern and western longitudes and the importance of snowmelt dominated systems that occur between the southern and northern latitudes (Wohl et al. 2016). Topographic surveys were conducted using a total station at the majority of sites and a real-time kinematic geographic position system at sites in California and Oklahoma. OHWM indicators were identified based upon a combination of morphologic, vegetative, and sediment indicators. The survey equipment was used to map channel geometry and the location of OHWM indicators. Along each cross section, detailed field notes were collected to document OHWM indicators. A Wolman (1954) pebble count of 300 pebbles was conducted at a majority of sites to characterize bed grain size. Additionally, photographs were collected to document the condition of the site and other features that would help post-process the data in the office.

Table 1. OHWM site locations, site codes for sites located on Figure 4 and survey dates.

Region	Sub-region	Watershed	Subbasin	Site Code	Survey Date
Northeast	Mid-Atlantic (M)	James River (JR)	Topopotomoy Creek (TP)	NEMJRTP	4/10/2017
	Mid-Atlantic (M)	James River (JR)	Rivanna River (RV)	NEMJRRV	4/13/2017
	North Carolina (NC)	Santee (ST)	Davidson River (DR)	SENCSTDR	3/15/2017
Southeast	North Carolina (NC)	Santee (ST)	Beetree Creek (BT)	SENCSTBT	3/16/2017
	South Carolina (SC)	Santee (ST)	Bush River (BR)	SESCSTBR	3/13/2017
Southern Prairies	Oklahoma (OK)	Red River (RR)	Cobb Creek (CC)	SPOKRRCC	1/30/2017
	Oklahoma (OK)	Red River (RR)	Mud Creek (MC)	SPOKRRMC	2/1/2017

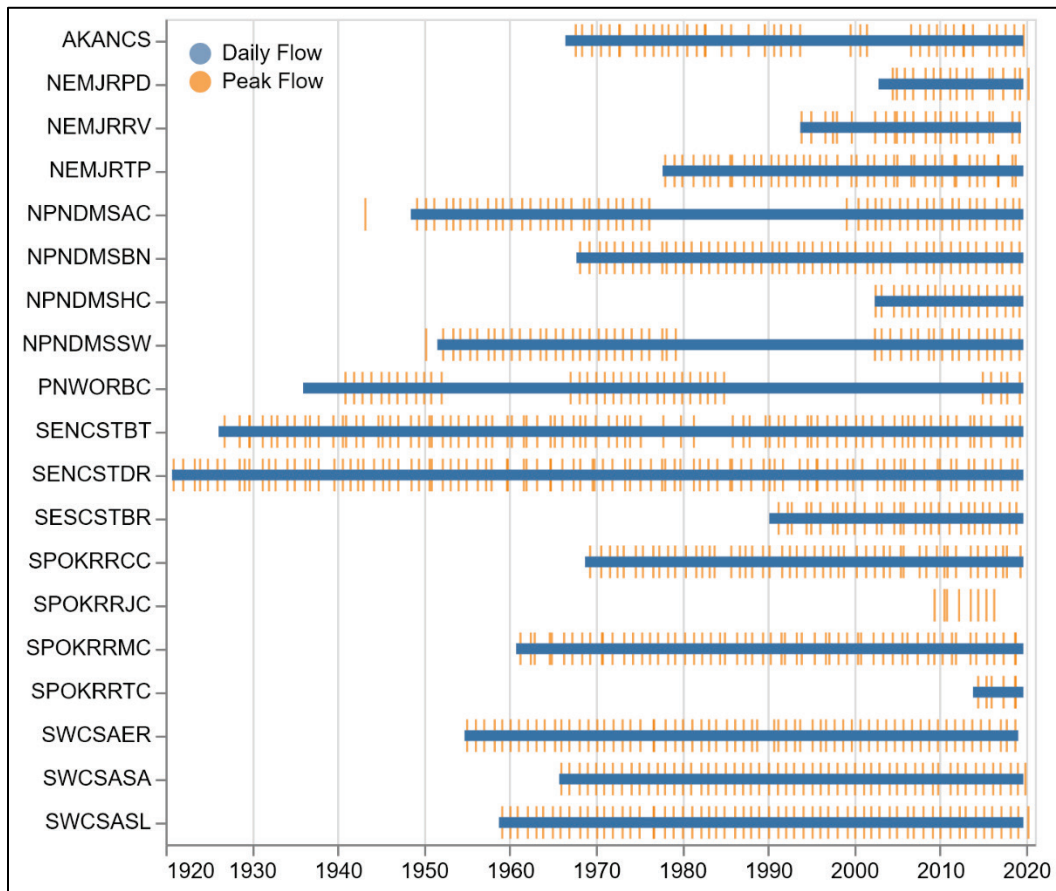
Region	Sub-region	Watershed	Subbasin	Site Code	Survey Date
Northern Prairies	North Dakota (ND)	Missouri River (MS)	Antelope Creek (AC)	NPNDMSAC	6/27/2017
	North Dakota (ND)	Missouri River (MS)	Burnt Creek (BN)	NPNDMSBN	6/29/2017
	North Dakota (ND)	Missouri River (MS)	Hay Creek (HC)	NPNDMSHC	6/26/2017
	North Dakota (ND)	Missouri River (MS)	Sweetwater Creek (SW)	NPNDMSSW	6/28/2017
Southwest	California (C)	Salinas (SA)	Estrella (ER)	SWCSAER	12/7/2017
	California (C)	Salinas (SA)	San Lorenzo (SL)	SWCSASL	12/12/2016
	California (C)	Salinas (SA)	San Antonio (SA)	SWCSASA	12/9/2016
Alaska	Anchorage (AN)		Chester Creek (CS)	AKANCS	8/14/2017

A site code was developed for each site that describes a site's geographical region, sub-region, watershed, subbasin as one- to two-letter abbreviations. For example, the site code NEMJRTP describes a site in the Northeast region, Mid-Atlantic sub-region, James River Watershed, and Totopotomoy Creek Subbasin.

4.2 Streamflow data

Daily river discharge and peak streamflow data were collected from the National Water Information System (NWIS 2020). The availability of peak streamflow data varies by location and river size. Streamflow is more commonly continuously gaged at larger rivers in more populated areas. Average daily streamflow is typically available for longer periods and is reported more consistently than peak streamflow data. Figure 12 shows the gaps in the peak streamflow record in some of the surveyed sites (Table 1) versus the much longer and more consistent daily flow records. Gaps in the data, or short records, caused four sites to be excluded from the study because the same analysis could not be applied to those sites. Therefore, NEMJRPD (Pedlar River), PNWORBC (Butte Creek), SPOKRRJC (Jimmy Creek), SPOKRRTC (Travertine Creek) were removed from the analysis. Because of the longer and consistent records of daily streamflow, the AM and POT analysis was conducted with these data.

Figure 12. Daily and peak streamflow period of record for OHWM survey sites. Gaps in the data, or particularly short records, meant that some of these sites were not suitable for the study (NEMJRPD, PNWORBC, SPOKRRJC, SPOKRRTC).



5 Hydrological Analysis of Ordinary High Water Mark (OHWM)

Hydrological processes create diverse physical indicators in a riverine environment that can aid the physical interpretation of the flooding regime of a river system. These physical indicators can be identified at frequently inundated portions of the banks of a river to the highest point in a river floodplain. Depending on the location of a physical indicator within a river valley, the temporal frequency and magnitude of flooding events can be estimated through a flood frequency analysis in rivers with systematic records of observed discharge. HWMs consistent with the OHWM definition can exist at different elevations within a cross section (i.e., left and right bank) and longitudinally (i.e., upstream and downstream) in a sequence of cross sections. Similar to bankfull, these physical indicators of high flow are likely formed by a range of high flow events and not just a single event. To better understand their magnitude and frequency of flows connected to forming these physical indicators, they are related to a flow at the elevation of the OHWM. The case study presented in this section demonstrates how flood frequency analysis can be used to understand the relationship of streamflow to field surveyed HWMs within a cross section and throughout a site.

5.1 Case study northeast

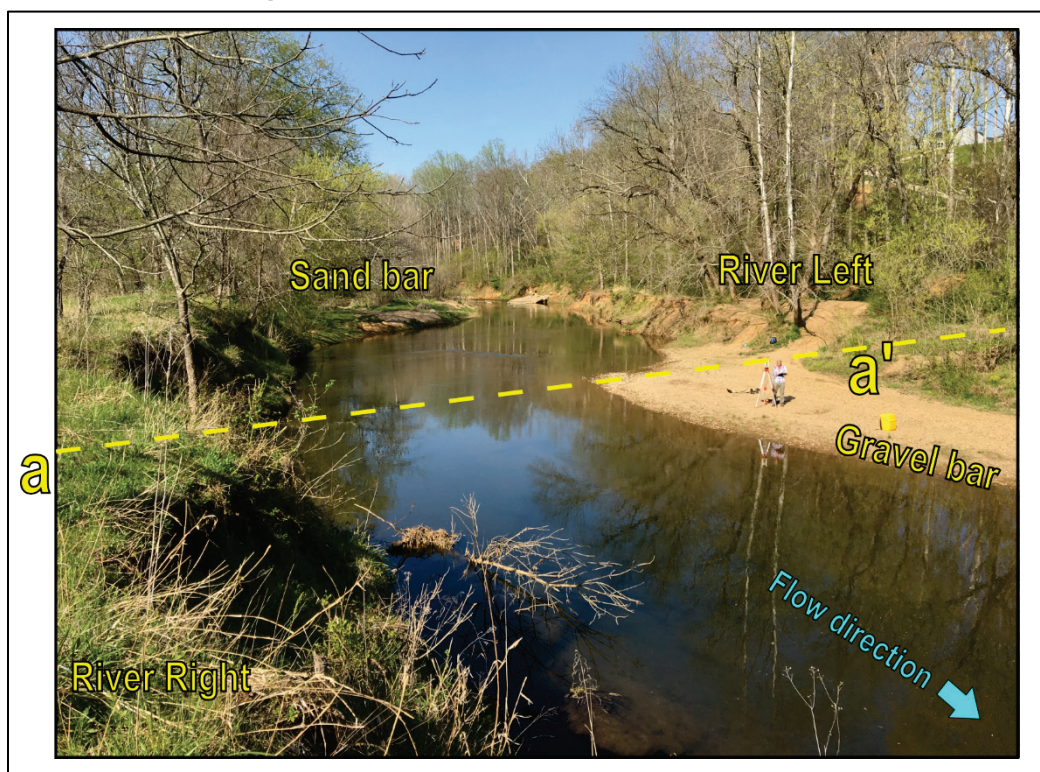
The Rivanna River OHWM site (NEMJRRV) is located in the Mid-Atlantic sub-region of the Northeast Region (Table 1). The survey was located immediately downstream of the USGS gauge 02032640 on the north fork of the Rivanna River near Earlysville, VA. The river originates in the Blue Ridge Mountains in the James River watershed with a 279 km² drainage area and topographic relief of 981 m. The National Land Cover Database (Yang et al. 2018) classifies the dominant land cover as forest (68%) and secondary land use as agriculture (23%) (Table 2).

Table 2. North Fork Rivanna River, VA, watershed characteristics.

Variable	Value	Units
Drainage Area	279	Square Kilometers
Sinuosity	1.33	–
Valley Width	83	Meters
Channel Width	41	Meters
Dominant Land Use	Forest (68%)	
Secondary Land Use	Agriculture (23%)	
Mean Annual Flow	3.69	Cubic Meters per second

The surveyed reach is located in a partially confined valley with a forested hillslope confining flow on the left and an open field on the right (Figure 13). Left and right is relative to the downstream direction in a river. The left bank of the survey site consisted of a deciduous trees slump toward the river. Although the right bank contained a few deciduous trees, it consists mainly of an actively maintained field. The riverbed is composed of gravel and sand deposits. There were alternating sand and gravel bars throughout the reach.

Figure 13. North Fork Rivanna River site photo.



An annual cyclic analysis of the average daily streamflow record shows seasonal variations (Figure 14). In general, streamflow increases in the fall and winter seasons and recedes to low flow during spring and summer months. The largest streamflow events occur in the spring and summer months, which leads to the largest variation in the observed record (Figure 15).

Figure 14. Average and median streamflow calculated over the period 1993–2020 for the North Fork Rivanna River USGS Gauge 02032640.

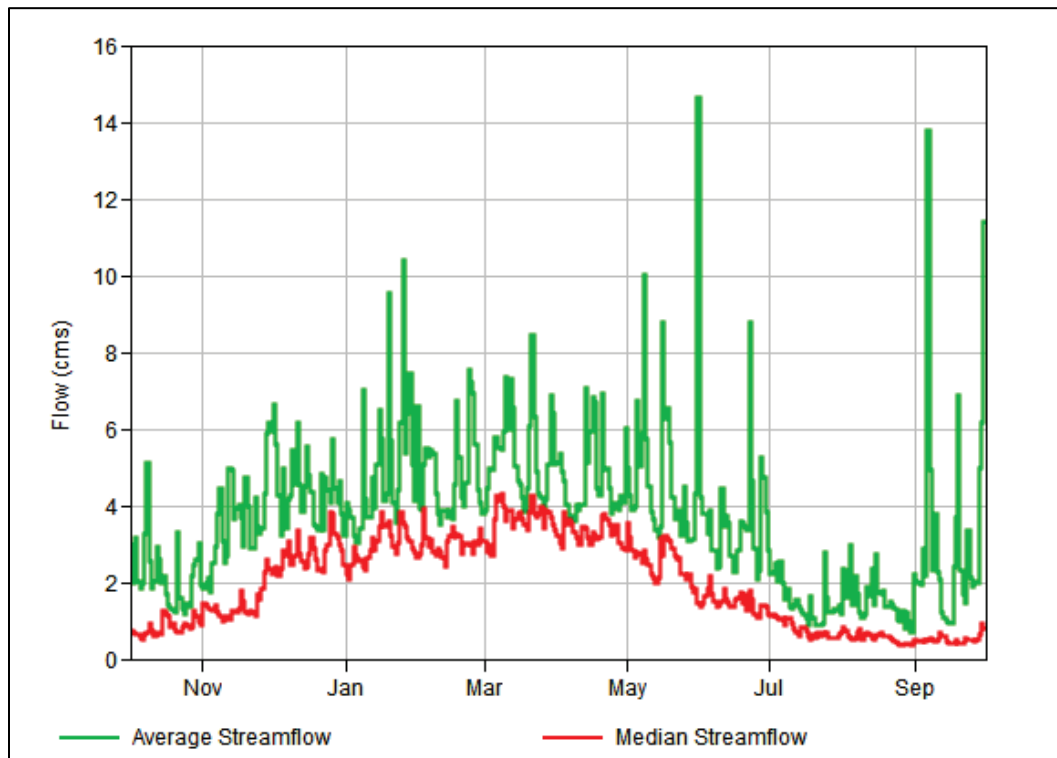
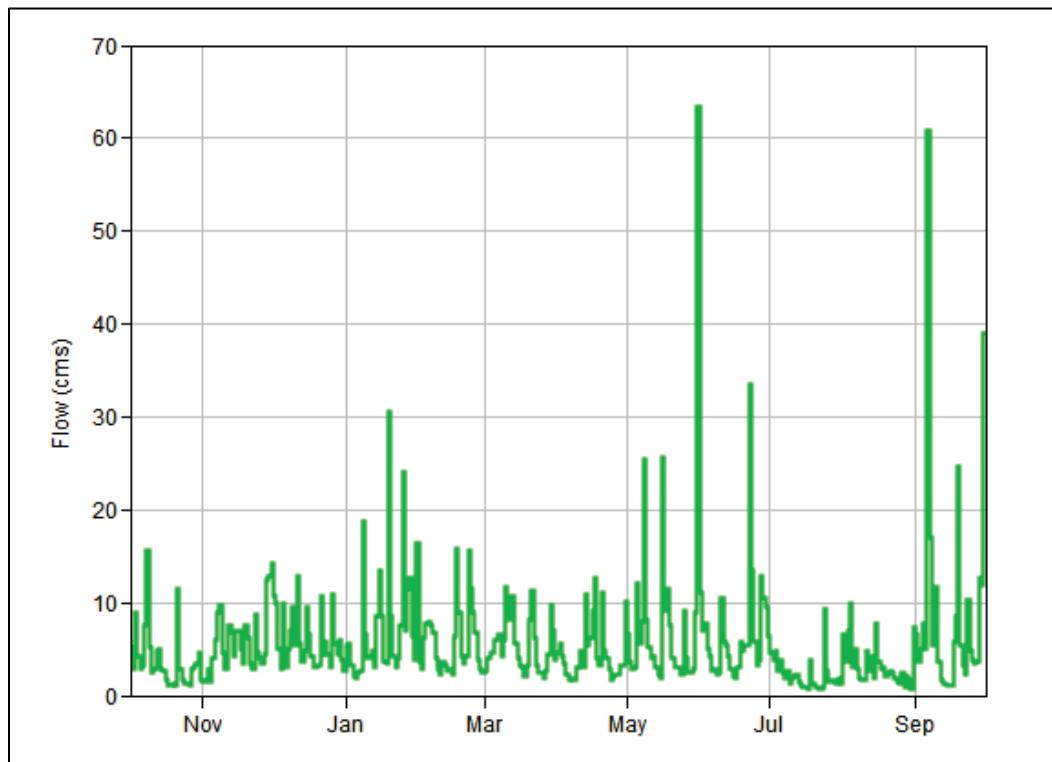


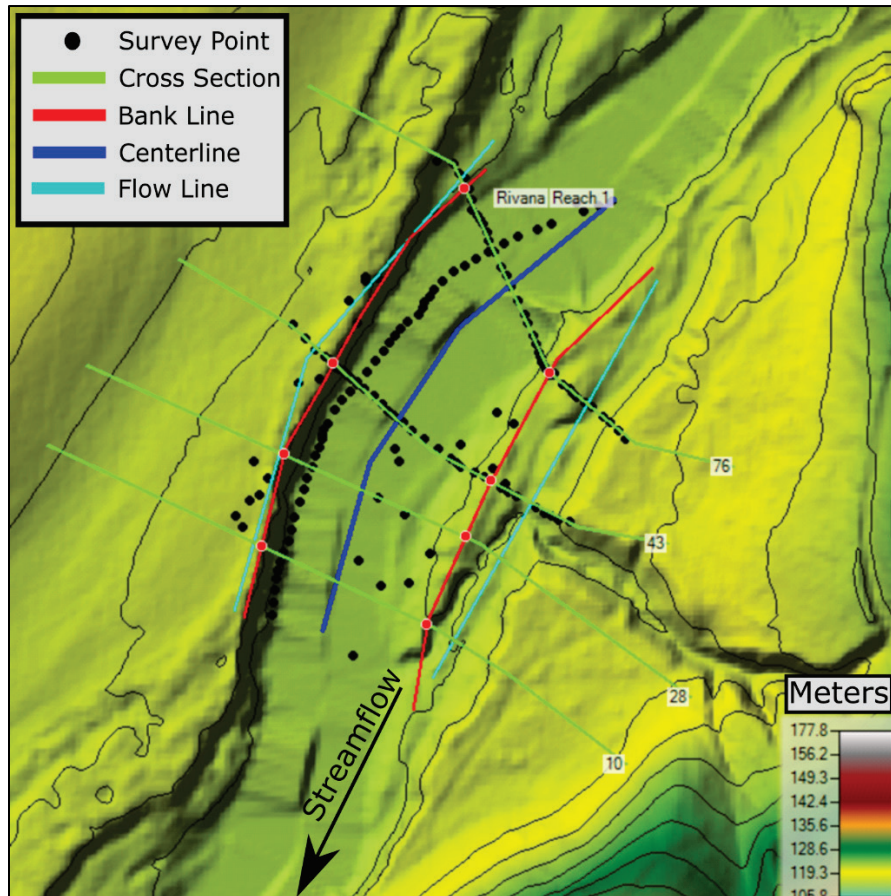
Figure 15. Streamflow standard deviation calculated over the period 1993–2020 for the North Fork Rivanna River USGS gauge 02032640.



5.1.1 Model description

The HEC-RAS model consisted of four cross sections spanning 73 m (Figure 16). The field survey consisted of two cross sections in the upstream extent of the models, a thalweg survey, and point observations of OHWM indicators between the two measured cross sections. The survey data were merged with the surrounding topography DEM in the UTM 17N (European Petroleum Survey Group 26917) projection. The bathymetry for the two downstream cross sections was interpolated based upon the channel slope calculated based on a 30 m line of 0.19%. Photographic guidance and field notes of riverbed sediment were used to calibrate the channel roughness coefficient with values ranging from 0.03 to 0.045. The slope used to interpolate the downstream cross sections was also used as the normal depth downstream boundary condition.

Figure 16. HEC-RAS model geometry for Rivanna River flow model. The survey points are shown as black points, and linear features represent the cross sections (green line), centerline (dark blue line), bank lines (red line), and flow lines (cyan line).



5.1.2 OHWM delineation

For the two surveyed cross sections, OHWM was identified based upon a combination of geomorphologic, vegetative, and sediment indicators (Figure 17 and Figure 18). OHWM was delineated at the interface of the gravel and point bar deposits and established woody vegetation. Immediately below the OHWM elevation, the sediment characteristics transitioned from gravel to clay. The woody vegetation was more abundant above the identified OHWM location and became sparse below that same elevation. The identifying features used to delineate the OHWM persisted across the entire site (upstream and downstream accounting for channel gradient).

Figure 17. Elevation of OHWM for XS1 at North Fork Rivanna River, VA.

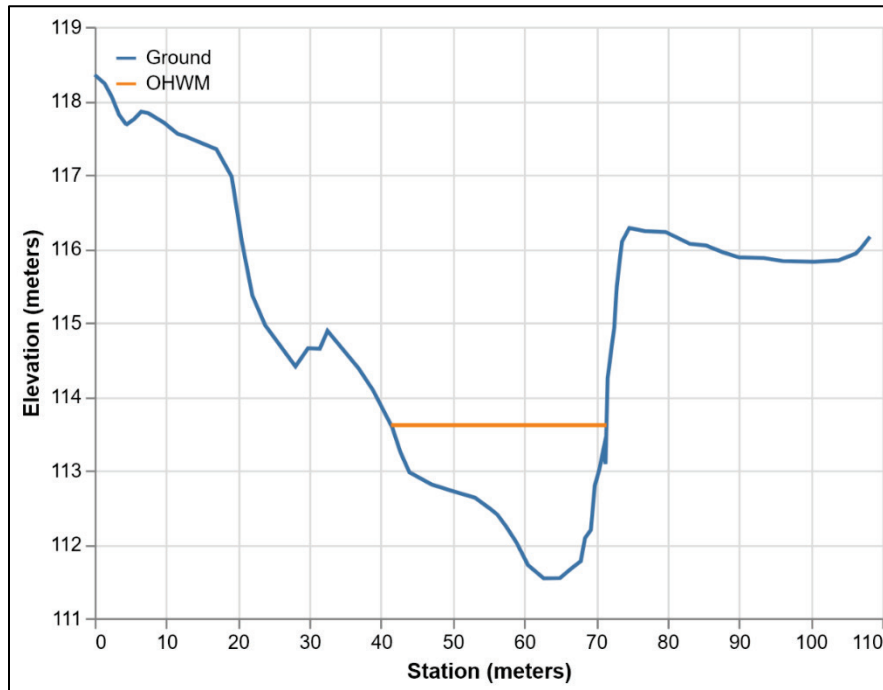
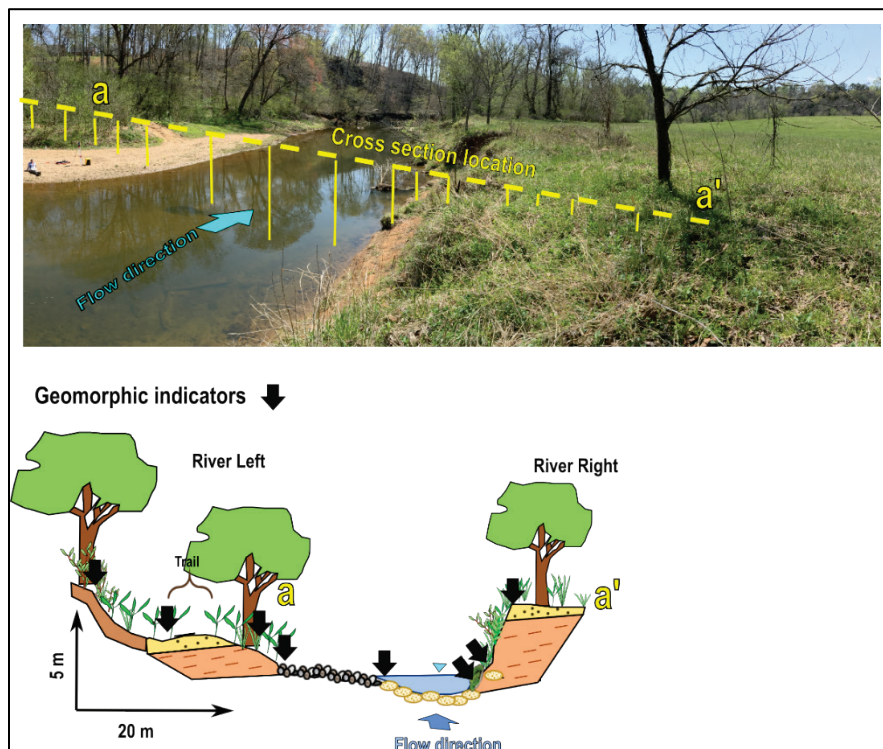


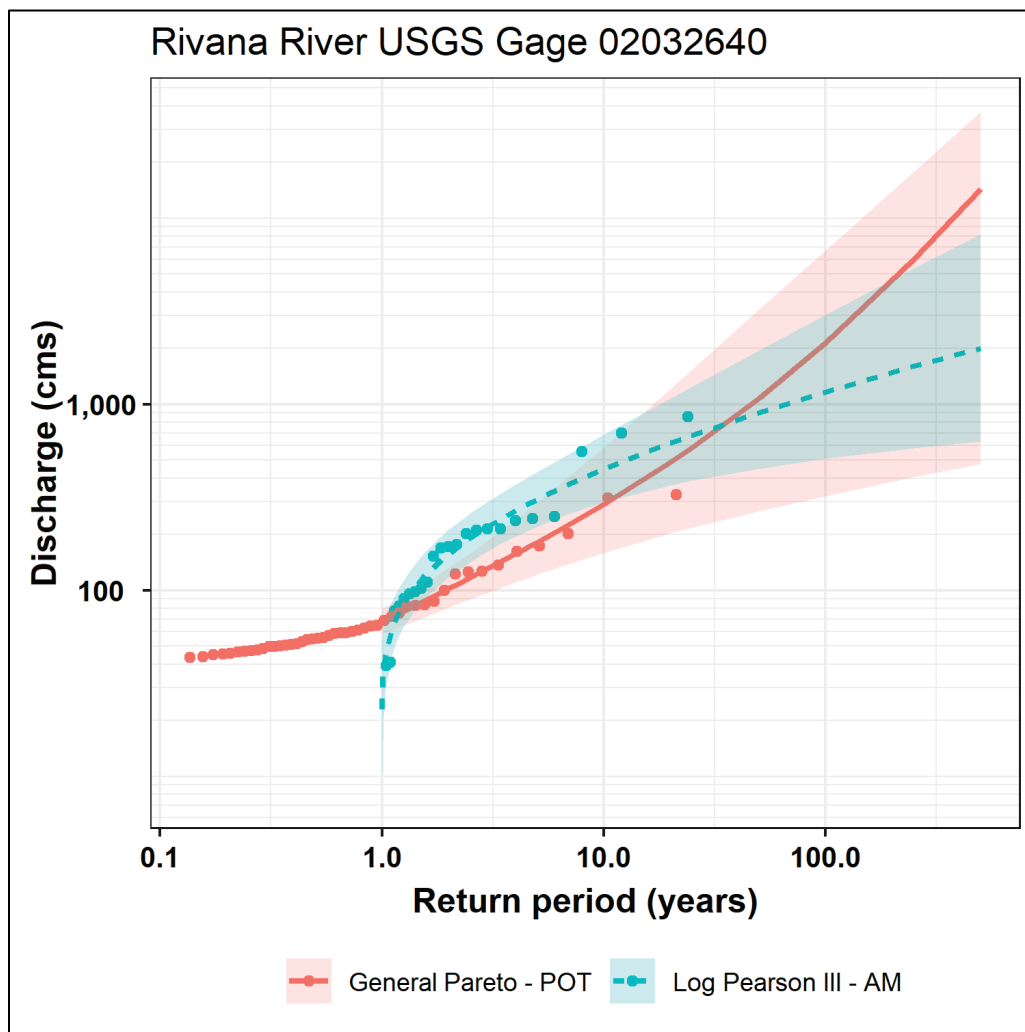
Figure 18. Location and elevation of potential indicators of OHW on surveyed cross section a-a' across the North Fork Rivanna River, VA. The shaded blue area in the cross section represents the water surface (denoted by an inverted blue triangle) during the day of the survey and is not indicative of high flow.



5.1.3 Results

The USGS streamgage at Rivanna River (USGS gauge 0203640) has daily and peak streamflow records beginning in 1993 for a total length of 26 and 23 yr, respectively (Figure 6). The flood frequency curves for the AM and POT methods are presented in Figure 19. The POT method resulted in lower magnitude relationships when compared to the AM flood frequency curve, but the confidence intervals between the two methods are overlapping.

Figure 19. Flood frequency curves based on AM and POT approaches for North Fork Rivanna River at USGS gage 02032640.



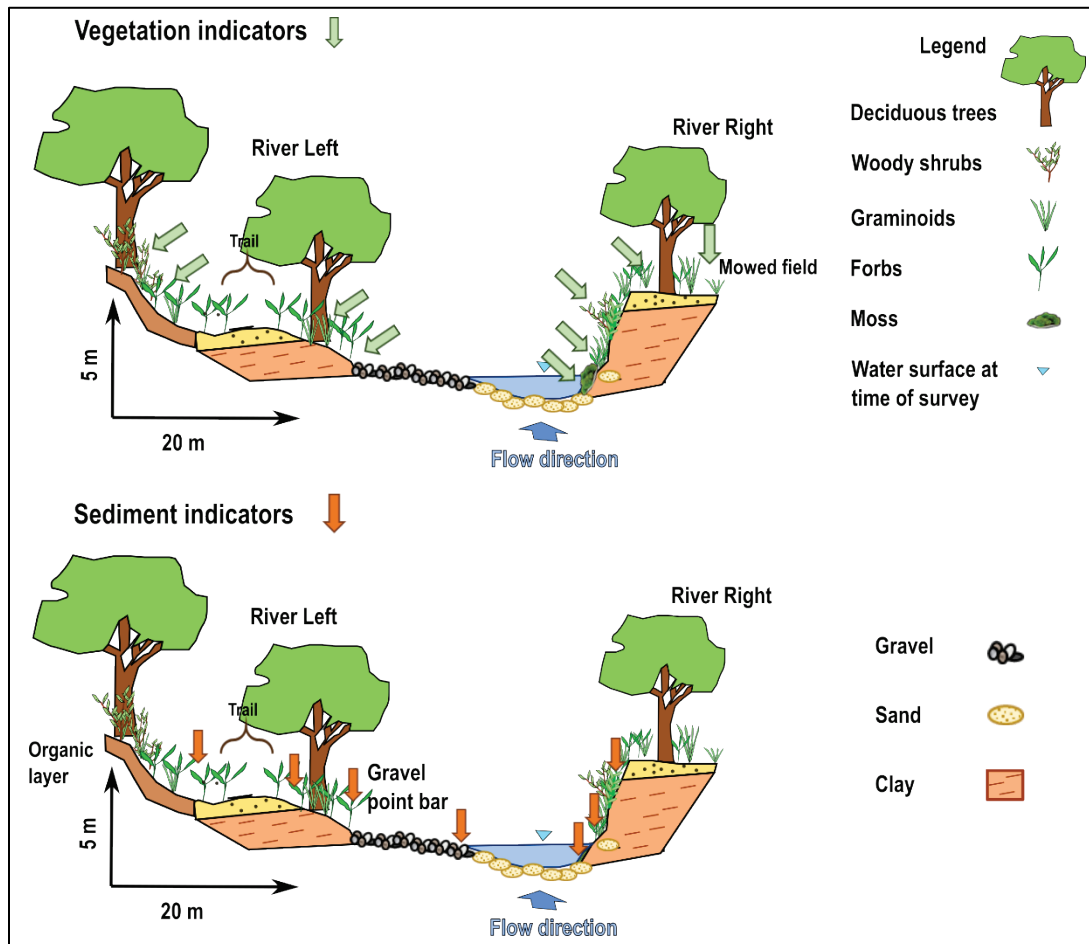
The AM and POT flood frequency curves were used to estimate the return period of corresponding to sediment and vegetative transitional features that were used to support the OHWM delineation (Figure 20). The AM and POT return periods corresponding to the elevation of the OHWM field indicators are presented in Table 3. The vegetative indicators had

return periods ranging from 0.13 to 5 yr and 1.003 to 2.24 yr for the POT and AM methods, respectively. The physical indicators had a large range of return periods with AM ranging from 1.002 and 2.24 and POT ranging from 0.13 to 5 yr.

Table 3. Return periods of the field identified OHWM indicators at Rivanna River Cross Section 1.

Type of HWM Indicator	Feature	Elevation (m)	Streamflow (cms/s)	POT Return Period (yr)	AM Return Period (yr)	Relative to OHWM
Vegetation	Moss	112.93	43.3	0.13	1.03	Below
	Herbaceous Vegetation	113.6	80.3	1.35	1.23	At
	Deciduous Trees	114.4	172.9	5.0	2.24	Above
Soil and sediment	Sand Gravel Transition	112.27	21.71	Below Threshold	1.002	Below
	Gravel Clay Transition	112.93	43.3	0.13	1.03	Below
	Clay Sand Transition	113.6	80.3	1.35	1.23	At
	Sand Clay Transition	114.4	172.9	5.0	2.24	Above

Figure 20. Rivanna River Cross Section 1 showing transition points for vegetation (top) and sediment (bottom). The water surface is the water surface during the day of the survey and is not indicative of high flow.



5.1.4 Implications of AM and POT flood frequency return periods

Direct comparisons between the AM and POT flood frequency methods have limited value for understanding the behavior of flooding events because they are formulated with different streamflow metrics. However, since the AM is the most accepted formulation for flood frequency it can be used to determine if the POT curve is characteristic of flood frequency analysis. An ideal flood frequency curve is one that has small uncertainty bands, has a gradually increasing trend with return interval, and continues to predict larger flooding events for longer return periods. The size of the uncertainty bands is directly correlated with how well the statistical distribution fits the sample of flooding events from the streamflow record. When distribution fitting parameters result in a curve that accurately represents the return interval and magnitude of observed flooding events, the uncertainty bands are small. The rate in which streamflow increases

with return interval is a function of the tails of the input distribution of observed peaks. Outliers (low or high) influence the tails of the distribution and can result in portions of the curve that rapidly increase. A flood frequency can become asymptotic for large flooding events when the input distribution has small variation between the largest peaks. An asymptotic curve would imply that streamflow remains constant with increasingly extreme hydrological events, which is not physically plausible.

Return periods from the POT and AM flood frequency can be compared if the POT return periods are converted to an annual time-step using Equation 6. A major difference between the two flood frequency methods is that POT curves can be used to quantify streamflow levels associated with return periods of less than 1 yr (Figure 9), which reduces the uncertainty in estimating magnitudes of small flooding events. Small flooding events are often describing flows that are still contained within the channel banks. Because POT incorporates smaller flood flows in its analysis, it was hypothesized that it would be able to better characterize flood frequency for flows connected to the OHWM. The near-vertical rising portion of the streamflow AM curve with return periods slightly greater than 1 yr is an artifact of the annual filter applied to the streamflow record. This results in a large range of flows that are all assigned very similar return periods. The POT flood frequency curve shows a more gradual increase in streamflow with return period estimates, reflecting more realistic estimation of the magnitude of these common events. The AM and POT curves intersect near the inflection point where the AM changes from rapid to gradual increases in streamflow magnitude.

5.2 Flood frequency of OHWM

The AM and POT return periods for the field delineated OHWM marks are described in Table 4. Cross sections with return periods larger than 15 yr are deemed to be outliers because POT is only applicative for short (e.g. < than 15 yr). A more robust outlier analysis is not supported by the sample size of data analyzed in this study. Nationally, OHWM is related to return periods 0.5 to 9.08 yr, and 1.05 to 11.01 yr for POT and AM flood frequency methods, respectively. The POT method produced return periods within the expected range up to 10 yr (Wohl et al. 2016) for all sites except for SENCSTDR and NPNDMSHC. The suspiciously large POT return periods for SENCSTDR (89 and 38 yr) are likely because the sample of peaks from the average daily streamflow record is not as representative as the 98 yr peak streamflow record for that site (Figure 5).

The peak streamflow record was sufficiently large that the AM methodology reasonably represented small to intermediate flooding events SENCSTDR. It is unusual to have sites with long records, but when they are available, then the AM method would be sufficient for these sites. The return periods (8.6 and 15.7 yr) at NPNDMSHC indicate the POT flood frequency systematically underestimated the magnitude of small to intermediate flooding events. The large variation in return periods at NPNDMSHC is likely related to the fact the site is located in an urban area with a flashy flow regime. The use of daily streamflow record for this site may have still underestimated the size of flows moving through this channel.

Table 4. POT and AM return period of OWHM. Outliers indicated by asterisk.

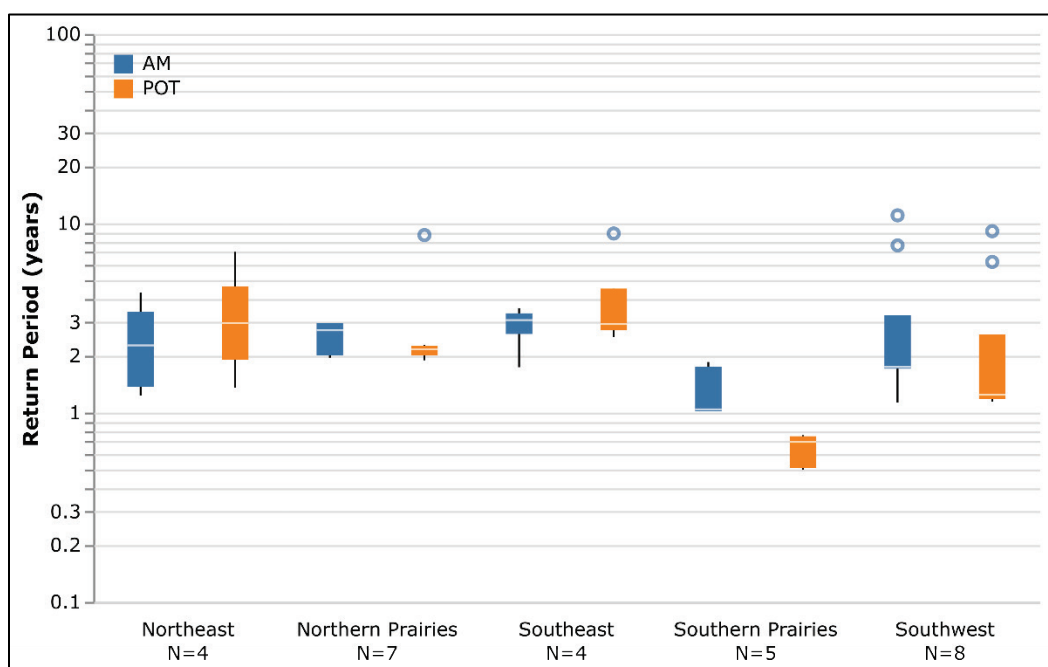
Stream	Drainage Area (km ²)	Cross Section	OWHM Elevation (m)	POT (yr)	AM (yr)	Streamflow (cms)
NEMJRRV	279.1	XS 1	113.6	1.35	1.23	80.03
		XS 2	114.1	2.09	1.41	103.28
NEMJRTP	66.62	XS 1	12.7	7.06	4.29	26.85
		XS 2	13.0	3.85	3.12	20.18
SENCSTBT	14.14	XS 1	822.6	8.83	2.89	8.82
		XS 2	822.7	3.08	1.737	5.65
SENCSTDR	104.3	XS 1	646.65	89.36*	7.54	138.39
		XS 2	646.61	38.86*	3.751	108.76
SENCSTBR	303.29	XS 1	111.9	2.79	3.57	89.2
		XS 2	111.9	2.5	3.27	85.38
SPOKRRCC	341.21	XS 1	421.2	0.51	1.02	20.5
		XS 2	421.2	0.5	1.02	20.69
		XS 3	421.5	0.75	1.04	19.91
SPOKRRMC	1488.45	XS 1	228.9	0.7	1.75	140
		XS 2	229.0	0.76	1.85	150.22
NPNDMSAC	614.26	XS 1	600.8	2.00	2.72	28.62
		XS 2	601.0	2.28	2.97	32.48
NPNDMSBN	285.7	XS 1	516.4	2.01	2.00	14.6
		XS 2	516.5	1.89	1.95	13.82
NPNDMSHC	82.39	XS 1	504.9	8.66	2.01	11.11
		XS 2	505.0	15.71*	2.39	12.73
NPNDMSSW	407.38	XS 1	576.1	2.22	2.97	28.15

Stream	Drainage Area (km ²)	Cross Section	OHWL Elevation (m)	POT (yr)	AM (yr)	Streamflow (cms)
		XS 2	576.1	2.16	2.97	27.56
SWCSAER	3466.57	XS 1	207.6	9.08	11.01	353.28
		XS 2	207.6	6.25	7.64	231.39
SWCSASA	558.14	XS 1	246.5	1.18	1.13	97.06
		XS 2	246.8	1.37	1.81	107.74
SWCSASL	604.04	XS 1	133.4	1.18	1.71	20.80
		XS 2	133.5	1.26	1.75	21.90
		XS 3	133.5	1.22	1.73	21.46
		XS 4	133.5	1.14	1.69	20.15
AKANCS	2.32	XS 1	6.14	3.74	1.66	4.68
		XS 2	6.13	3.61	1.6	4.60
			Average	2.9	2.6	

The large variation in the Southeast can be attributed to the poor performance of the POT methodology at SENCSTDR. The other two remaining sites in the Southeast region (SENCSTBT and SENCSTBR) had return periods that were systematically higher than the AM return periods. The Southern Prairies region highlight the advantages of using POT flood frequency over AM. The AM return periods for the two sites range from 1.02 to 1.85 yr. An AM return interval of 1.02 yr is near the theoretical minimum of 1.01 yr. POT return periods indicate that OHWM is related to return periods ranging from 0.5 to 0.76 yr. Therefore, the POT method allowed an estimation of these small-frequent floods (i.e., high flows).

The regional OHWM flood frequency relationships are depicted in Figure 21. Regionally, the AM and POT methodologies produced similar return periods for all regions except for the Southeast and Southern Prairies. The sample size is small for each region for a more in-depth analysis, but the data provide understanding of general trends and possible differences between regions. These results agree with the general consensus described in Wohl et al. (2016). Based on the sample of sites analyzed, OHWM is related to small-frequent flooding events. A more robust regional analysis would be required to determine if other factors influence the relationship between OHWM and streamflow.

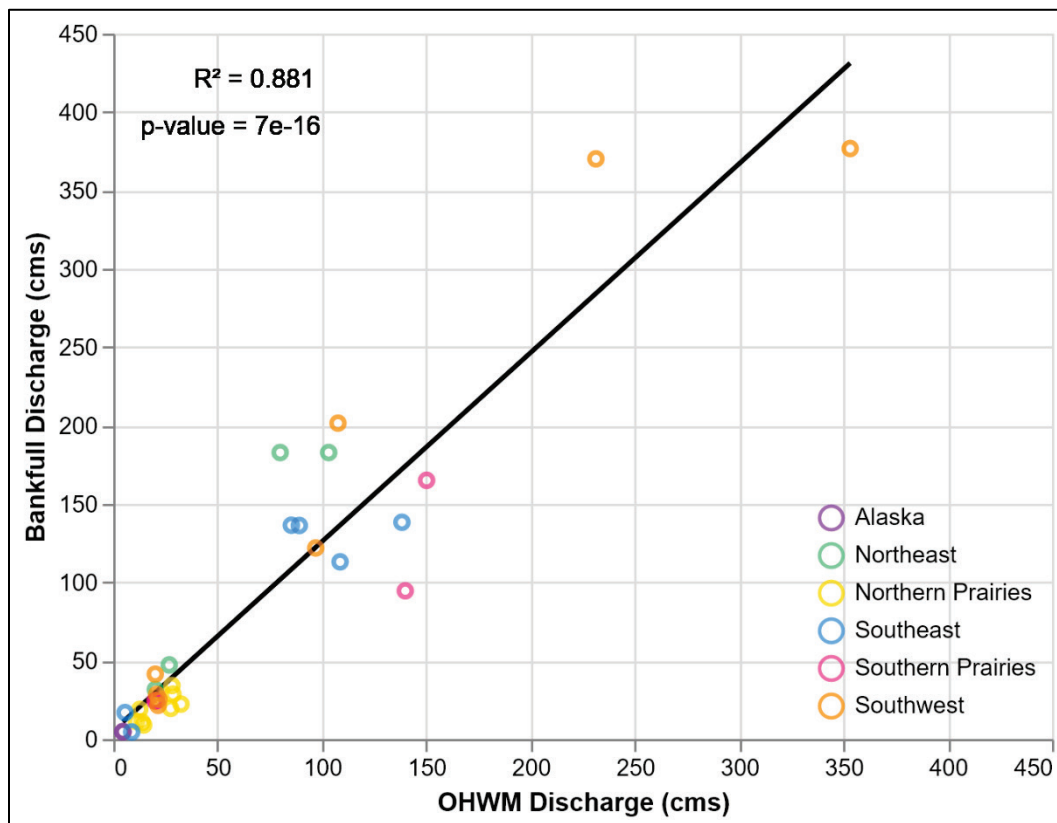
Figure 21. Regional OHWM flood frequency return period boxplot. Outliers removed from Table 4 have been eliminated.



5.3 Relationships between bankfull discharge and OHWM

The hydraulic flow models were used to determine constant level discharges associated with field delineated bankfull and OHWM elevations. Bankfull elevations for each cross section were delineated using channel morphology with an emphasis placed on identifying inflection points in bank slopes from larger to smaller. The modeled discharges produced a statistically sufficient positive correlation between OHWM and bankfull discharge, with bankfull discharge generally being larger than OHWM (Figure 22). The within-region variation increases around the relationship with increasing drainage area (Table 4). The POT outliers are included in this comparison of bankfull and OHWM discharge because the hydraulic models were not affected by the large return periods. Figure 22 demonstrates at-a-site variability, which was much more pronounced in streams with discharges greater than 100 cms.

Figure 22. Discharge relationship between field-delineated OHWM and bankfull elevations. Each data point represents a field surveyed cross section and is color coded based on geographic region.



At-a-site variation was evident in both OHWM and bankfull characteristics. For instance, the sites located in the Southwest region (SWCSASA and SWCSAER) demonstrate cross section-to-cross section variability in field-identified OHWM at one site and bankfull discharges at a different site. Some of the cross-sectional variability in OHWM and bankfull at SWCSASA is due to the braided river system at this site. The surveyed cross sections had considerable differences in length, where the upstream cross section is located in an area where the system was in a deeper, narrower main channel thread and the downstream cross section was located in a relatively unconfined area where the system extended across multiple threads. The change in cross section to cross section morphology resulted in OHWM and bankfull being associated with different levels of streamflow. In contrast to SWCSASA, SWCSAER is located in an engineered channel with leveed banks. The levees resulted in nearly identical bankfull elevations and a larger variation in the identified OHWM elevations. OHWM varied between cross sections because the vegetation on the channel banks appeared to be influenced by the

irrigation from surrounding agricultural fields. The at-a-site variability is expected because HWM are likely formed by a variety of high flows, not one single flow. The root mean square error for the regression is 40.7 cms. This analysis was applied to sites that were just upstream or downstream of USGS streamgages. These streamgages tend to be in locations where the channel has a simplistic morphology. Therefore, more work will need to be done to understand relationships between bankfull and OHWM in streams with complicated morphologies.

6 Summary

We investigated how magnitude-frequency metrics of the middle-upper end of the flow spectrum can be used to describe Ordinary High Water Mark (OHWM) using a field dataset of topographic surveys of rivers instrumented with streamgages. The frequency and magnitude of streamflow were related to field-delineated OHWM indicators using annual maximum and partial duration flood frequency methods. Based on our results, the data do not suggest that there is a specific return period that can be applied to any given location in the country. Return periods ranged between 0.5 to 9.08 yr for peaks-over-threshold (POT) and 1.02 to 11.01 yr for annual maximum (AM), with three outliers greater than 15 yr at two of the sites for POT method. Furthermore, there was at-a-site variability between cross sections.

Overall, the two flood frequency methods produced similar return periods for OHWM, with POT able to better quantify the frequency of small magnitude floods, particularly <1 yr recurrence intervals. The recurrence interval of a flow that would leave physical indicators related to OHWM is specific to reach, watershed, and regional characteristics. Therefore, flood frequency analyses of the middle-upper end of the flow spectrum do not prove to be a robust metric for final identification of the location of the OHWM but can be useful in providing supporting evidence for defining where OHW will exist in channel. Streamgage data, with a long enough record, would need to be available at a site to apply this method. A much larger sample of regionally specific data will need to be collected, to develop regional relationships that allow prediction of OHW return periods in ungauged basins. The POT method can be useful for streams with shorter streamgage records or to assist in characterizing small flood flows under a 1 yr return period interval. Ultimately, flood frequency analysis needs to be combined with flow modeling to provide a water surface elevation for the high flows. To narrow down the elevation of the OHWM, flood frequency analysis can be used to provide an upper and lower bound of these high flows. This can then be paired with field evidence to provide support for the location of the OHWM.

The results of this study show how magnitude-frequency streamflow relationships can be used to better define the frequency of OHWM. The flood frequency analysis can provide supporting evidence for identifying locations of the upper and lower bounds for large-infrequent flooding, as

well as the locations of channel-forming small-frequent flooding along a reach. We found a positive correlation between OHWM and bankfull discharge, which presents a linkage between the indicators used to identify the OHWM and geomorphologic features that characterize bankfull elevation. Therefore, more recent scientific methods developed to identify bankfull can also assist with OHWM identification in every region of the country. Averages are often used when characterizing bankfull discharge and width and do not inherently incorporate site variability. Differences in substrate, vegetation, valley confinement can all lead to variability in channel width, flow depth, and velocity which can result in variability in the high flows that leave persistent flow indicators that are identified as the OHWM. Therefore, the recurrence intervals at the identified elevation of the OHWM along a stream reach may be within a range of recurrence intervals and not just one specific number. Figure 21 demonstrates at-a-site variability, which was much more pronounced in streams with discharges greater than 100 cms. Therefore, flood frequency analysis can help identify the range of flows that may include the OHWM, narrowing down the location of the OHWM, but a single discharge or recurrence interval should not be used to represent the OHWM. Future work should focus on further characterization of the variability in high flows at sites and how that is linked to formation of different high water marks.

References

- Andrews, E. D. 1986. "Downstream Effects of Flaming Gorge Reservoir on the Green River, Colorado and Utah." *Geological Society of America Bulletin* 97(8): 1012. [https://doi.org/10.1130/0016-7606\(1986\)97<1012:deofgr>2.0.co;2](https://doi.org/10.1130/0016-7606(1986)97<1012:deofgr>2.0.co;2).
- Askquith, W. 2020. *lmomco—L-moments, Censored L-moments, Trimmed L-moments, L-comoments, and Many Distributions*. R Package version 2.3.6. <https://rdr.io/cran/lmomco/>
- Bader, Brian, and Jun Yan. 2016. *eva: Extreme Value Analysis with Goodness-of-Fit Testing*. R Package version 0.2.4. <https://rdr.io/cran/eva/>
- Barnes, Harry Hawthorne. 1967. "Roughness Characteristics of Natural Channels." *Water Supply Paper*. Vol. Water Supp. Denver. Washington, DC: United States Government Printing Office. <https://doi.org/10.3133/wsp1849>.
- Beechie, T., J. S. Richardson, A. M. Gurnell, and J. Negishi. 2012. "Watershed Processes, Human Impacts, and Process-Based Restoration." *Stream and Watershed Restoration: A Guide to Restoring Riverine Processes and Habitats*. Chichester, West Sussex : John Wiley & Sons, Ltd. <https://doi.org/https://doi.org/10.1002/9781118406618.ch2>.
- Bjerklie, David M., Delwyn Moller, Laurence C. Smith, and S. Lawrence Dingman. 2005. "Estimating Discharge in Rivers Using Remotely Sensed Hydraulic Information." *Journal of Hydrology* 309(1–4): 191–209. <https://doi.org/10.1016/j.jhydrol.2004.11.022>.
- Bradley, J. B., and D. B. Simons. 1990. "Delineation of Ordinary High Water." In *Hydraulic Engineering, Proceedings of the 1990 National Conference*, 1164–1167. New York: American Society of Civil Engineers.
- Brunsdon, D., and J. B. Thornes. 1979. "Landscape Sensitivity and Change." *Transactions of the Institute of British Geographers* 4(4): 463. <https://doi.org/10.2307/622210>.
- Castellarin, Attilio, Silvia Kohnová, Ladislav Gaál, A. Fleig, J. L. Salinas, A. Toumazis, Thomas Kjeldsen, and Neil Macdonald. 2012. *FLOODFREQ COST Action ES0901: European Procedures for Flood Frequency Estimation: Review of Applied-Statistical Methods for Flood-Frequency Analysis in Europe: WG2*. (NERC) Centre for Ecology & Hydrology. <https://www.cost.eu/wp-content/uploads/2018/07/FLOODFREQ-COST%20Action%20ES0901.pdf>.
- Castro, Janine M., and Philip L. Jackson. 2001. "Bankfull Discharge Recurrence Intervals and Regional Hydraulic Geometry Relationships: Patterns in the Pacific Northwest, USA." *Journal of the American Water Resources Association* 37 (5): 1249–62. <https://doi.org/10.1111/j.1752-1688.2001.tb03636.x>.
- Choulakian, V., and M. A. Stephens. 2001. "Goodness-of-Fit Tests for the Generalized Pareto Distribution." *Technometrics* 43(4): 478–84. <https://doi.org/10.1198/00401700152672573>.

- Chow, V. T. 1959. *Open Channel Hydraulics*. New York: McGraw-Hill Book Company, Inc.
- Claps, P., and F. Laio. 2003. "Can Continuous Streamflow Data Support Flood Frequency Analysis? An Alternative to the Partial Duration Series Approach." *Water Resources Research* 39(8): 1–11. <https://doi.org/10.1029/2002WR001868>.
- Coles, Stuart. 2013. *An Introduction to Statistical Modeling of Extreme Values*. Guildford, England: Springer. <https://doi.org/10.1007/978-1-4471-3675-0>.
- Curtis, K. E., R. W. Lichvar, and L. E. Dixon. 2011. *Ordinary High Flows and the Stage-Discharge Relationship in the Arid West Region*. ERDC/CRREL TR-11-12. Hanover, NH: US Army Engineer Research and Development Center.
- David, Gabrielle C. L., Ellen Wohl, Steven E. Yochum, and Brian P. Bledsoe. 2011. "Comparative Analysis of Bed Resistance Partitioning in High-Gradient Streams." *Water Resources Research* 47 (7). <https://doi.org/10.1029/2010wr009540>.
- Einstein, H. A., and N. L. Barbarossa. 1952. "River Channel Roughness. *Trans. Am. Soc. Civ. Eng.* 117(1): 1121–1146.
- England, John F., Jr., Timothy A. Cohn, Beth A. Faber, Jerry R. Stedinger, Wilbert O. Thomas Jr., Andrea G. Veilleux, Julie E. Kiang, and Robert R. Mason, Jr. 2019. "Guidelines for Determining Flood Flow Frequency—Bulletin 17C." *Techniques and Methods*. Reston, VA: US Geological Survey. <https://doi.org/10.3133/tm4b5>.
- Gartner, John D., Matthew Mersel, Lindsey Lefebvre, and Robert Lichvar. 2016a. *The Benefits and Limitations of Hydraulic Modeling for Ordinary High Water Mark Delineation*. ERDC/CRREL TR-16-1. Hanover, NH: US Army Engineer Research and Development Center. <https://hdl.handle.net/11681/21574>.
- Gartner, John D., Matthew Mersel, and Robert Lichvar. 2016b. *Hydrologic Modeling and Flood Frequency Analysis for Ordinary High Water Mark Delineation*. ERDC/CRREL TR-16-2. Hanover, NH: US Army Engineer Research and Development Center. <https://hdl.handle.net/11681/21573>.
- Gilleland, Eric, and Richard W. Katz. 2016. "extRemes 2.0: An Extreme Value Analysis Package in R." *Journal of Statistical Software* 72 (8). <https://doi.org/10.18637/jss.v072.i08>.
- Harkins, Joe R., and Mark E. Green. 1981. *Depth Estimation for Ordinary High Water of Streams in the Mobile District of the US Army Corps of Engineers, Alabama and Adjacent States*. USGS Open-File Report 81-481. Tuscaloosa, AL: United States Department of the Interior, Geological Survey. <https://doi.org/10.3133/ofr81481>.
- Helsel, D. R., R. M. Hirsch, K. R. Ryberg, S. A. Archfield, and E. J. Gilroy. 2020. *Statistical Methods in Water Resources: US Geological Survey Techniques and Methods*. Book 4, chapter A3. <https://doi.org/10.3133/tm4a3>. [Supersedes USGS Techniques of Water-Resources Investigations, book 4, chapter A3, version 1.1.] Reston, VA: US Geological Survey.
- Johnson, Peggy A., and Thomas M. Heil. 1996. "Uncertainty in Estimating Bankfull Conditions." *Journal of the American Water Resources Association* 32(6): 1283–91. <https://doi.org/10.1111/j.1752-1688.1996.tb03497.x>.

- Junk, W. L., P. B. Bayley, and R. E. Sparks. 1989. "The Flood Pulse Concept in River-Floodplain Systems." Edited by D. P. Dodge, 110–127. *Proceedings of the International Large River Symposium, Canadian Special Publication of Fisheries and Aquatic Sciences*. Ottawa, Ontario: Department of Fisheries and Oceans.
- Krstolic, Jennifer L. 2007. *Bankfull Regional Curves for Streams in the Non-Urban, Non-Tidal Coastal Plain Physiographic Province, Virginia and Maryland*. Reston, VA: US Geological Survey. <https://lccn.loc.gov/2007473463>.
- Langbein, B. 1949. "Annual Floods and the Partial-Duration Flood Series." *Eos, Transactions American Geophysical Union* 30(6): 879–81. <https://doi.org/10.1029/TR030i006p00879>.
- Langousis, Andreas, Antonios Mamalakis, Michelangelo Puliga, and Roberto Deidda. 2016. "Threshold Detection for the Generalized Pareto Distribution: Review of Representative Methods and Application to the NOAA NCDC Daily Rainfall Database." *Water Resources Research* 52(4): 2659–81. <https://doi.org/10.1002/2015WR018502>.
- Leopold, Luna Bergere, and Thomas Maddock Jr. 1953. "The Hydraulic Geometry of Stream Channels and Some Physiographic Implications." Professional Paper 252. Reston, VA: US Geological Survey. <https://doi.org/10.3133/pp252>.
- Leopold, Luna B., and Herbert E. Skibitzke. 1967. "Observations on Unmeasured Rivers." *Geografiska Annaler: Series A, Physical Geography* 49(2–4): 247–255. <https://doi.org/10.2307/520892>.
- Leopold, L. B., W. G. Wolman, and J. P. Miller. 1964. *Fluvial Processes in Geomorphology*. San Francisco, CA: W. H. Freeman.
- Lichvar, R. W., David C. Finnegan, Michael P. Ericsson, and Walter Ochs. 2006. *Distribution of Ordinary High Water Mark (OHWM) Indicators and Their Reliability in Identifying the Limits of "Waters of the United States" in Arid Southwestern Channels*. ERDC/CRREL TR 06-05. Hanover, NH: US Army Engineer Research and Development Center. <http://hdl.handle.net/11681/5327>.
- Lichvar, R. W., and J. S. Wakeley. 2004. *Review of Ordinary High Water Mark Indicators for Delineating Arid Streams in the Southwestern United States*. ERDC TR-04.1. Hanover, NH: US Army Engineer Waterways Experiment Station, Environmental Laboratory.
- Lichvar, R. W., and S. M. McColley. 2008. *A Field Guide to the Identification of the Ordinary High Water Mark (OHWM) in the Arid West region of the Western United States: A Delineation Manual*. ERDC/CRREL TR 08-12. Hanover, NH: US Army Engineer Research and Development Center. <http://hdl.handle.net/11681/5308>.
- Madsen, Henrik, Peter F. Rasmussen, and Dan Rosbjerg. 1997. "Comparison of Annual Maximum Series and Partial Duration Series Methods for Modeling Extreme Hydrologic Events: 1. At-Site Modeling." *Water Resources Research* 33(4): 747–57. <https://doi.org/10.1029/96WR03848>.

- Mersel, M. K., and R. W. Lichvar. 2014. *A Guide to Ordinary High Water Mark (OHWM) Delineation for Non-Perennial Streams in the Western Mountains, Valleys, and Coast Region of the United States*. ERDC/CRREL TR-14-13. Hanover, NH: US Army Engineer Research and Development Center.
- Nanson, G. C., and J. C. Croke. 1992. "A Genetic Classification of Floodplains." *Geomorphology* 4: 459–486.
- NWIS (National Water Information System). 2019. National Water Information System Data Available on the World Wide Web (USGS Water Data for the Nation). Reston, VA: US Geological Survey. <https://doi.org/10.5066/F7P55KJN>.
- Olden, Julian D., and N. L. Poff. 2003. "Redundancy and the Choice of Hydrologic Indices for Characterizing Streamflow Regimes." *River Research and Applications* 19(2): 101–21. <https://doi.org/10.1002/rra.700>.
- Poff, N. LeRoy, J. David Allan, Mark B. Bain, James R. Karr, Karen L. Prestegard, Brian D. Richter, Richard E. Sparks, and Julie C. Stromberg. 1997. "The Natural Flow Regime." *BioScience* 47(11): 769–84. <https://doi.org/10.2307/1313099>.
- R Core Team. 2020. *R: A Language and Environment for Statistical Computing*. R Foundation for Statistical Computing, Vienna, Austria. URL <http://www.R-project.org/>.
- Roni, Philip, and Tim Beechie, eds. 2012. *Stream and Watershed Restoration*. Hoboken, NJ: John Wiley & Sons, Ltd. <https://doi.org/10.1002/9781118406618>.
- RStudio Team. 2020. *RStudio: Integrated Development for R*. RStudio, PBC, Boston, MA. <http://www.rstudio.com/>.
- Sherwood, James M., and Carrie A. Huitger. 2005. *Ohio. Department of Transportation, United States Federal Highway Administration, and US Geological Survey. Bankfull Characteristics of Ohio Streams and Their Relation to Peak Streamflows*. Reston, VA: US Geological Survey. <https://lccn.loc.gov/2005452568>.
- Stedinger, Jerry R., Richard M. Vogel, and Efi Foufoula-Georgiou. 1993. "Frequency Analysis of Extreme Events." *Handbook of Hydrology*. Edited by David R. Maidment, 10th-07–0397 ed., 39723. New York: McGraw-Hill.
- USACE (US Army Corps of Engineers). 2005. *Ordinary High Water Mark Identification*. USACE Regulatory Guidance Letter (RGL) 05-05. <http://www.nap.usace.army.mil/Portals/39/docs/regulatory/rgls/rgl05-05.pdf>.
- USACE, Institute for Water Resources Hydrologic Engineering Center. 2016. *Hydraulic Reference Manual* Davis, CA.
- Williams, Garnett P. 1978. "Bank-Full Discharge of Rivers." *Water Resources Research* 14(6): 1141–54. <https://doi.org/10.1029/wr014i006p01141>.

- Wohl, Ellen, Matthew K. Mersel, Aaron O. Allen, Ken M. Fritz, Steven L. Kichefski, Robert W. Lichvar, Tracie-lynn Nadeau, Brian J. Topping, Patrick H. Trier, and Forrest B. Vanderbilt. 2016. *Synthesizing the Scientific Foundation for Ordinary High Water Mark Delineation in Fluvial Systems*. SR-16-5. Hanover, NH: US Army Engineer Research and Development Center, Cold Regions Research and Engineering Laboratory.
- Wolman, M. G. 1954. "A Method for Sampling Coarse River-Bed Material." *Eos. Trans. AGU* 35: 951–956.
- Wolman, M. G., and L. B. Leopold. 1957. *River Flood Plains: Some Observations on Their Formation*. US Geological Survey Professional Paper 282-C. Reston, VA.
- Wolman, M. Gordon, and John P. Miller. 2021. "Magnitude and Frequency of Forces in Geomorphic Processes." *The Journal of Geology* 68(1) (1960): 54–74. Accessed March 10, 2021. <http://www.jstor.org/stable/30058255>.
- Yang, Limin, Suming Jin, Patrick Danielson, Collin Homer, Leila Gass, Stacie M. Bender, Adam Case, et al. 2018. "A New Generation of the United States National Land Cover Database: Requirements, Research Priorities, Design, and Implementation Strategies." *ISPRS Journal of Photogrammetry and Remote Sensing* 146(December): 108–23. <https://doi.org/10.1016/j.isprsjprs.2018.09.006>.
- Yochum, Steven E., Brian P. Bledsoe, Gabrielle C.L. David, and Ellen Wohl. 2012. "Velocity Prediction in High-Gradient Channels." *Journal of Hydrology* 424–425(6): 84–98. <https://doi.org/10.1016/j.jhydrol.2011.12.031>.
- Yochum, Steven E., Francesco Comiti, Ellen Wohl, Gabrielle C. David, and Luca Mao. 2014. *Photographic Guidance for Selecting Flow Resistance Coefficients in High-Gradient Channels*. RMRS-GTR-323. Fort Collins, CO: US Department of Agriculture, Forest Service, Rocky Mountain Research Station.

Acronyms and Abbreviations

AM	Annual Maximum
DEM	Digital Elevation Model
FPOT	Filtered Peaks Over Threshold
GIS	Geographic Information System
GOF	Goodness-of-Fit
GP	General Pareto
HEC-RAS	Hydrologic Engineering Center River Analysis Software
HWM	High Water Mark
LP3	Log Pearson 3
MAF	Mean Annual Flow
OHWM	Ordinary High Water Mark
POT	Peaks Over Threshold
USGS	US Geological Survey
UTM	Universal Transverse Mercator
XS	Cross Section

Unit Conversion Factors

Multiply	By	To Obtain
feet	0.3048	meters
cubic feet	0.02831685	cubic meters
feet	0.3048	meters
square miles	2.589998 E+06	square meters

REPORT DOCUMENTATION PAGE					Form Approved OMB No. 0704-0188	
<p>The public reporting burden for this collection of information is estimated to average 1 hour per response, including the time for reviewing instructions, searching existing data sources, gathering and maintaining the data needed, and completing and reviewing the collection of information. Send comments regarding this burden estimate or any other aspect of this collection of information, including suggestions for reducing the burden, to Department of Defense, Washington Headquarters Services, Directorate for Information Operations and Reports (0704-0188), 1215 Jefferson Davis Highway, Suite 1204, Arlington, VA 22202-4302. Respondents should be aware that notwithstanding any other provision of law, no person shall be subject to any penalty for failing to comply with a collection of information if it does not display a currently valid OMB control number.</p> <p>PLEASE DO NOT RETURN YOUR FORM TO THE ABOVE ADDRESS.</p>						
1. REPORT DATE August 2021		2. REPORT TYPE Final Report		3. DATES COVERED (From - To)		
4. TITLE AND SUBTITLE Hydrologic Analysis of Field Delineated Ordinary High Water Marks for Rivers and Streams				5a. CONTRACT NUMBER		
				5b. GRANT NUMBER		
				5c. PROGRAM ELEMENT NUMBER		
6. AUTHOR(S) Daniel Hamill and Gabrielle C. L. David				5d. PROJECT NUMBER		
				5e. TASK NUMBER		
				5f. WORK UNIT NUMBER		
7. PERFORMING ORGANIZATION NAME(S) AND ADDRESS(ES) Cold Regions Research and Engineering Laboratory US Army Engineer Research and Development Center 72 Lyme Road Hanover, NH 03755-1290				8. PERFORMING ORGANIZATION REPORT NUMBER ERDC/CRREL TR-21-9		
9. SPONSORING/MONITORING AGENCY NAME(S) AND ADDRESS(ES) Wetland Regulatory Assistance Program US Army Corps of Engineers Vicksburg, MS 39180-6933				10. SPONSOR/MONITOR'S ACRONYM(S) WRAP		
				11. SPONSOR/MONITOR'S REPORT NUMBER(S)		
12. DISTRIBUTION/AVAILABILITY STATEMENT Approved for public release; distribution is unlimited.						
13. SUPPLEMENTARY NOTES Funding Account Code U4375873; AMSCO Code 088893						
14. ABSTRACT Streamflow influences the distribution and organization of high water marks along rivers and streams in a landscape. The federal definition of ordinary high water mark (OHWM) is defined by physical and vegetative field indicators that are used to identify inundation extents of ordinary high water levels without any reference to the relationship between streamflow and regulatory definition. Streamflow is the amount, or volume, of water that moves through a stream per unit time. This study explores regional characteristics and relationships between field-delineated OHWMs and frequency-magnitude streamflow metrics derived from a flood frequency analysis. The elevation of OHWM is related to representative constant-level discharge return periods with national average return periods of 6.9 years using partial duration series and 2.8 years using annual maximum flood frequency approaches. The range in OHWM return periods is 0.5 to 9.08, and 1.05 to 11.01 years for peaks-over-threshold and annual maximum flood frequency methods, respectively. The range of OHWM return periods is consistent with the range found in national studies of return periods related to bankfull streamflow. Hydraulic models produced a statistically significant relationship between OHWM and bank-full, which reinforces the close relationship between the scientific concept and OHWM in most stream systems.						
15. SUBJECT TERMS Floodplains, Hydrologic models, Rivers, Streamflow, Water levels						
16. SECURITY CLASSIFICATION OF:			17. LIMITATION OF ABSTRACT	18. NUMBER OF PAGES	19a. NAME OF RESPONSIBLE PERSON	
a. REPORT	b. ABSTRACT	c. THIS PAGE			Daniel Hamill	
Unclassified	Unclassified	Unclassified	SAR	62	19b. TELEPHONE NUMBER (Include area code) 603-646-4240	

